EUROPEAN COMMISSION
DIRECTORATE-GENERAL
Joint Research Centre

Institute for Environment and Sustainability

Numerical weather simulations in support to the CCU CAML Lidar measurements: Preliminary results for the case study of 21st September 2006

S. Potempski[1], F. Barnaba[2] and S. Galmarini[1]

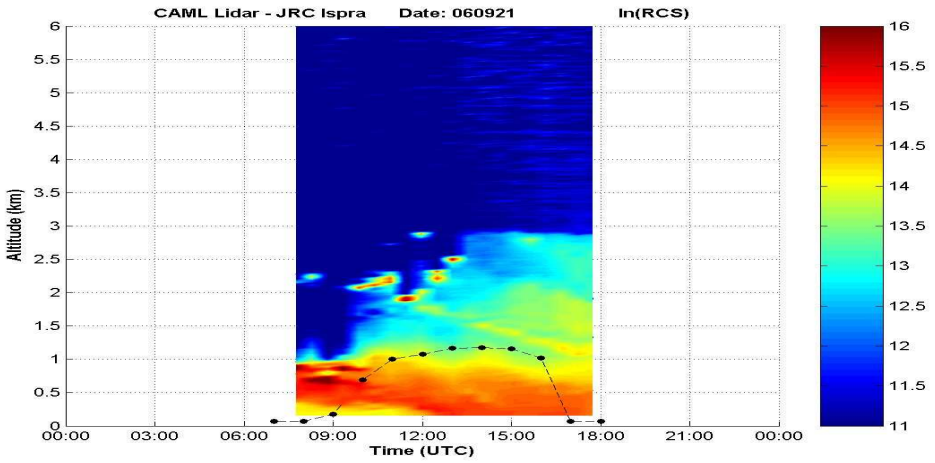

European Commission - DG Joint Research Centre,
Institute for Environment and Sustainability,
(1) Transport and Air Quality and (2) Climate Change Units
IT-21020 Ispra (VA), Italy

2007

EUR 22855 EN

The mission of the Institute for Environment and Sustainability is to provide scientific-technical support to the European Union's Policies for the protection and sustainable development of the European and global environment.

European Commission
Directorate-General Joint Research Centre
Institute for Environment and Sustainability

Contact information

Dr. S. Potempski
JRC/IES/TAQU
TP 441
Joint Research Centre
21020 Ispra
Italy
slawomir.potempski@jrc.it
Tel. +39 0332 789944
Fax. +39 0332 785466

Dr. F. Barnaba
JRC/IES/CCU
TP 290
Joint Research Centre
21020 Ispra
Italy
francesca.barnaba@jrc.it
Tel. +39 0332 785202
Fax. +39 0332 785704

Dr. S. Galmarini
JRC/IES/TAQU
TP 441
Joint Research Centre
21020 Ispra
Italy
stefano.galmarini@jrc.it
Tel. +39 0332 785382
Fax. +39 0332 785466

http://ies.jrc.cec.eu.int/
http://www.jrc.cec.eu.int

EUR 22855 EN

ISSN 1018-5593

Luxembourg: Office for Official Publications of the European Communities

Printed in Italy

EUROPEAN COMMISSION
DIRECTORATE-GENERAL
Joint Research Centre

Institute for Environment and Sustainability

Numerical weather simulations in support to the CCU CAML Lidar measurements: Preliminary results for the case study of 21st September 2006

S. Potempski[1], F. Barnaba[2] and S. Galmarini[1]

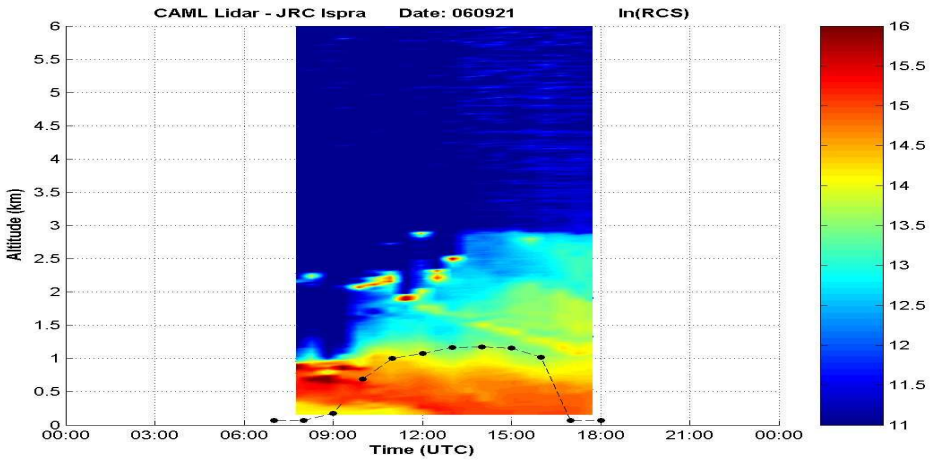

European Commission - DG Joint Research Centre,
Institute for Environment and Sustainability,
[1]Transport and Air Quality and [2]Climate Change Units
IT-21020 Ispra (VA), Italy

2007

Content

1. Introduction

On 21st September the CCU-CAML lidar at Ispra performed measurements of aerosol vertical profiles between 8.00 and 10.00 UTC (see Fig. 1).

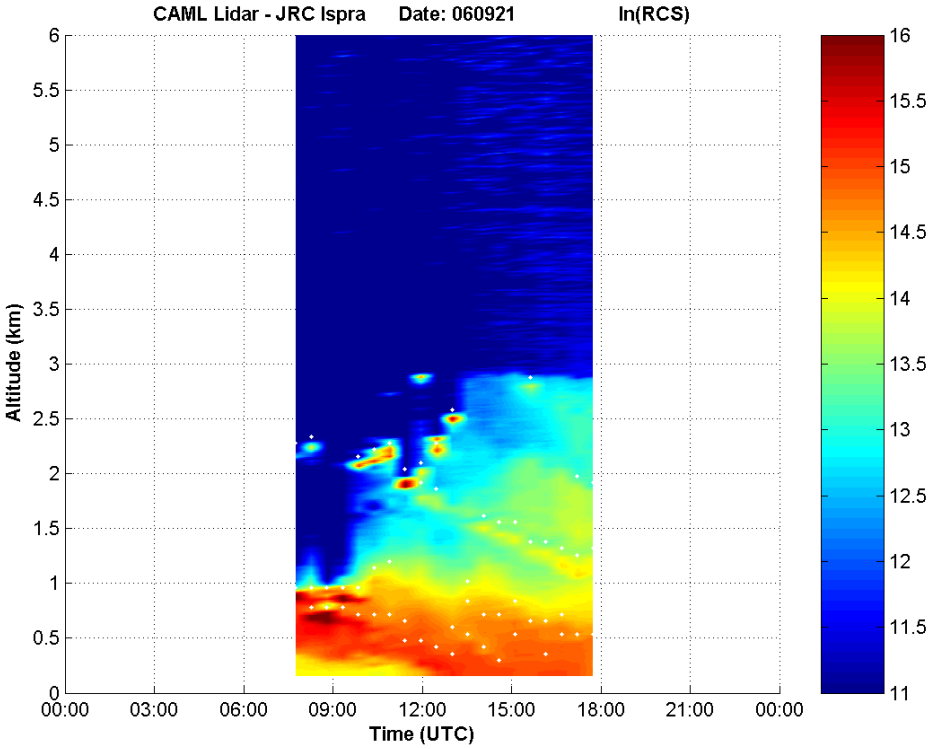

Fig. 1 Range corrected lidar signal (RCS) showing the daily variability of the aerosol vertical distribution on 21.09.2006

Quite high values of aerosols concentration were registered up to about 1 km altitude during the day. Interestingly, the lidar revealed a descent of the highest aerosol loads towards the ground during the morning. Corresponding to this descent, particulate matter (PM) mass measurements performed at the JRC-EMEP station revealed a doubling of PM10 levels at the ground (Fig. 2).

A series of numerical simulations were performed (using the weather numerical mesoscale model MM5 in high resolution) to understand to which extent the lidar-detected evolution of the particles distribution along the vertical could be explained by the boundary layer and/or horizontal transport processes. A particular stress was put on investigation of boundary layer parameters.

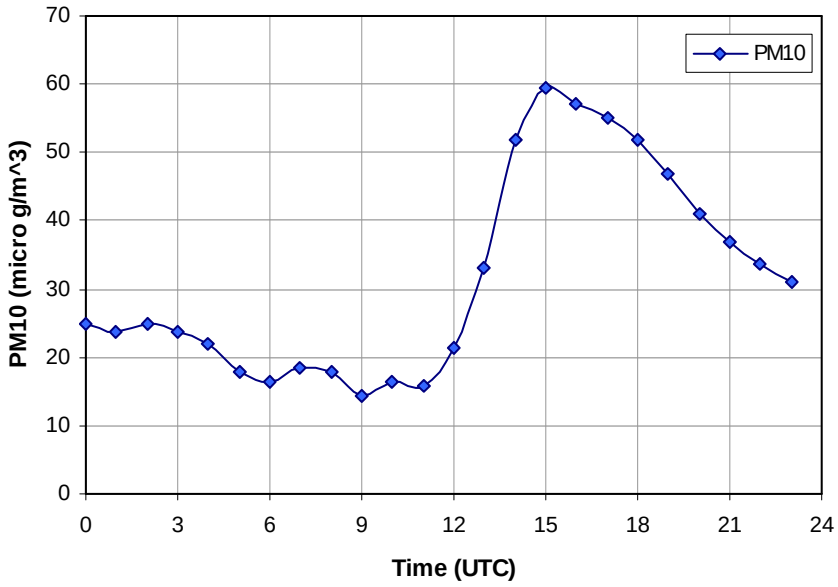

Fig. 2 Daily variability of the aerosol mass (PM10, $\mu g/m^3$) as recorded at the JRC-EMEP station on 21.09.2006

2. Configuration of the simulation domains.

In order to investigate the boundary layer development, three simulations were performed using the MM5 code [1, 2]. The configuration of the domains was as follows:

- the central point was put at the location (8.6E, 45.8N),
- four nested domains with two-way option were used with grid steps respectively: 27 km, 9 km, 3 km and 1 km in both directions,
- the sizes of the domains were approximately: 2160 km, 1080 km, 486 km and 180 km,
- the nested domains were located centrally in the mother domains (Fig. 3).

The USGS datasets for elevation, land use, vegetation and soil data were applied with the following resolutions: 10 min (~ 19 km), 5 min (~ 9 km), 2 min (~ 4 km) and 30 sec (~ 0.9 km) for the defined four domains respectively.

The vegetation/land use data for the finest domain is shown on Fig. 4 below. The white spots on the picture correspond to glacier or ice/snow cover. The biggest red one in bottom part of the picture indicates the city of Milan.

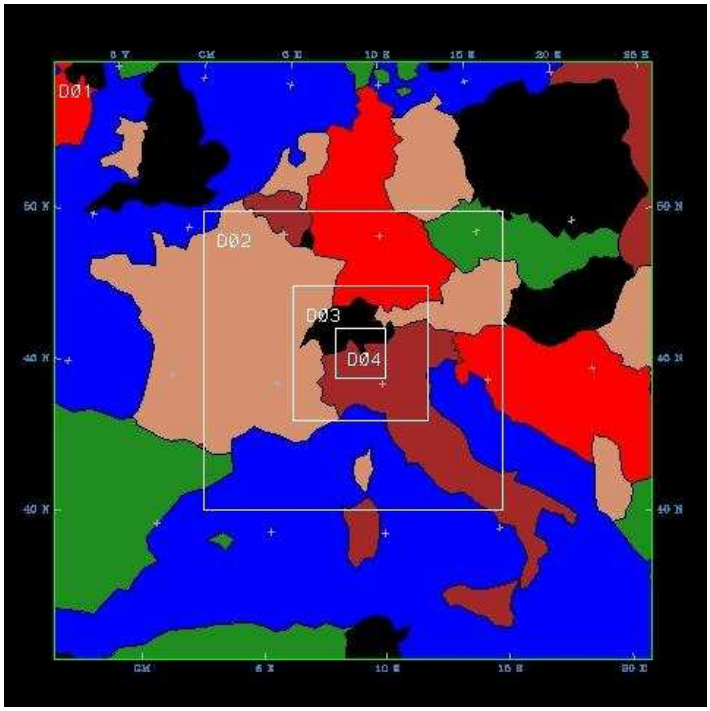

Fig. 3 Four nested domains used in MM5 simulations

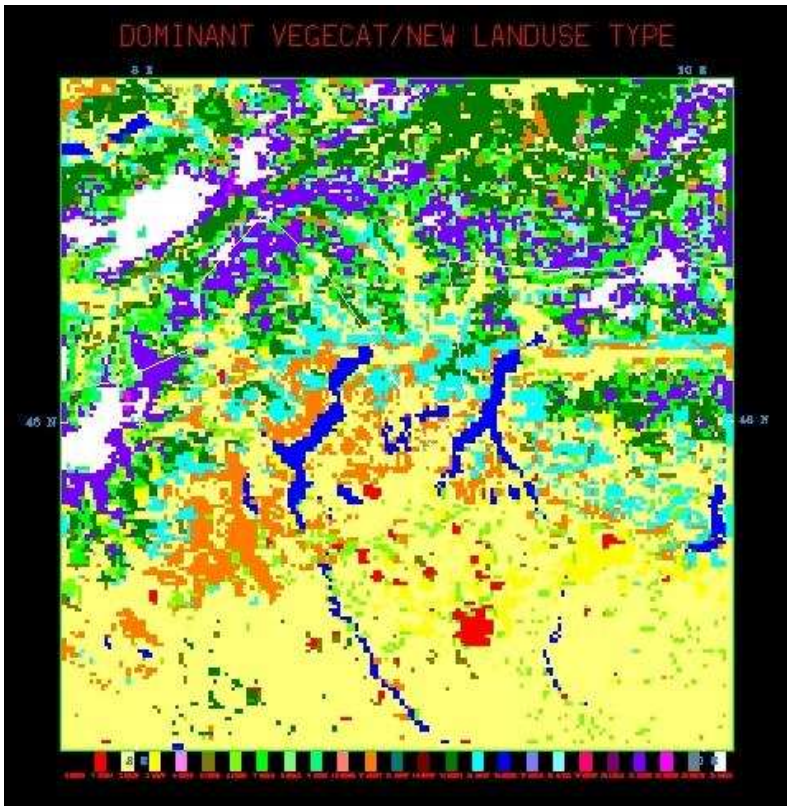

Fig. 4 Land use/vegetation data for the fourth domain

3. Configuration of MM5 runs

The ECMWF data were used to establish initial and boundary conditions for MM5 runs. The meteorological datasets for the period from 19th September to 21st

September contained all the typical necessary data together with soil and snow data. Thus four main meteorological datasets were created by preparatory MM5 module called *pregrid*:

- obligatory meteorological data (wind, humidity, temperature, geopotential, etc.),
- sea surface temperature data,
- snow data,
- soil data,

with the resolution of time step set as 3 hours.

These datasets were further combined with the terrain data for all the domains to create initial and boundary conditions on the grids defined for each domain for the period of simulations.

The following configuration parameters were used in MM5 runs:

- Schultz microphysics;
- Kain-Fritsch cumulus parameterization (new version) for the biggest domain, Grell parameterization for domain 2 and 3, no cumulus for the finest grid;
- Three different MM5 simulations were performed with three different boundary layer schemes:
    - High-resolution Blackadar scheme,
    - Scheme used in Eta model (Mellor-Yamada),
    - Scheme used in NCEP MRF model (Hong-Pan).

The applied boundary layer schemes were chosen to be appropriate for high-resolution simulations.

All the simulations were organized as follows:

- simulation for the biggest domain started for the day 19 September (hour 0.00),
- simulations for the nested domain started with some delay related to the mother domain: domain 2 started 12 hours later than domain 1, domain 3 12 hours later than domain 2 and domain 4 18 hours later than domain 3 (i.e. on 20th September at 18.00).

4. Simulations results

As stated above three main simulations were made with three different boundary layer schemes. The results of all the simulation were transformed into GrADS (Grid Analysis and Display System) package via standard tools available with MM5.

The following three variables were particularly investigated:

- boundary layer height,
- sensible heat flux,
- friction velocity.

In the following three pictures (Figs. 5-7) time series of boundary layer height are shown using the following colours:

black - Ispra station (the nearest grid point), green - average over space grid (~1km) at Ispra, cyan - average north of Ispra, red - average south of Ispra, magenta - average west of Ispra and blue - average east of Ispra.

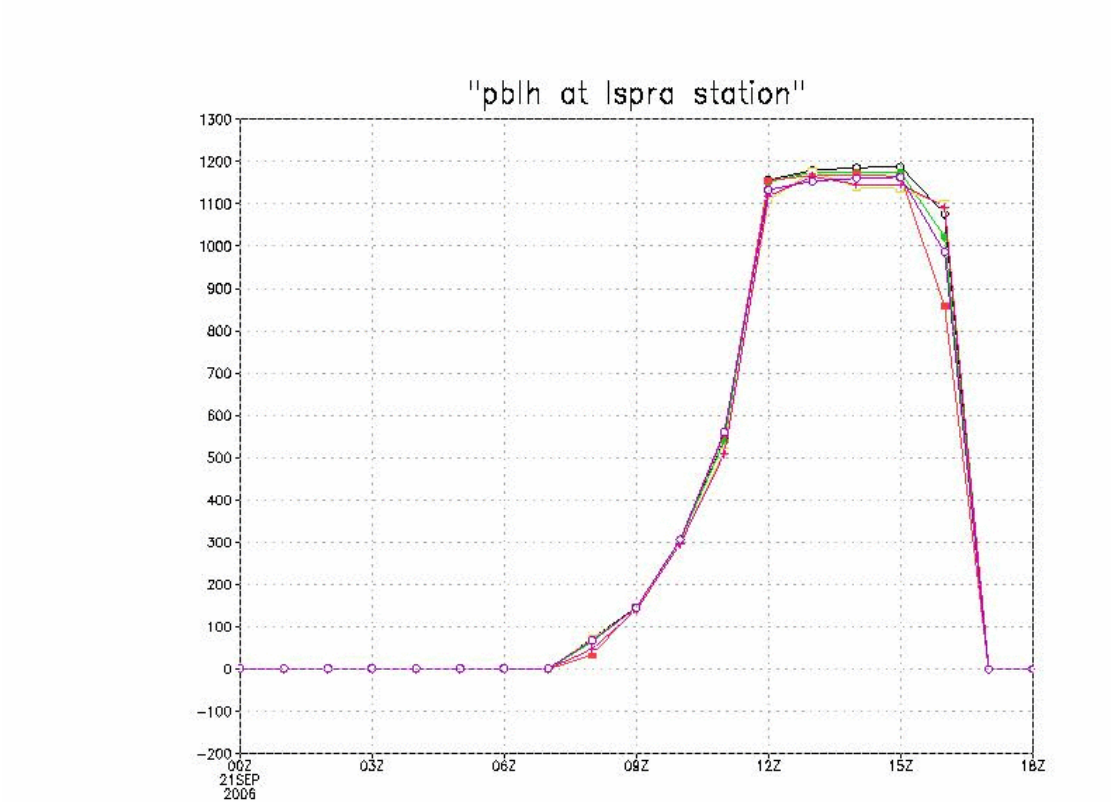

Fig. 5 Boundary layer height: Blackadar scheme (x-axis: UTC time, y-axis: height [m])

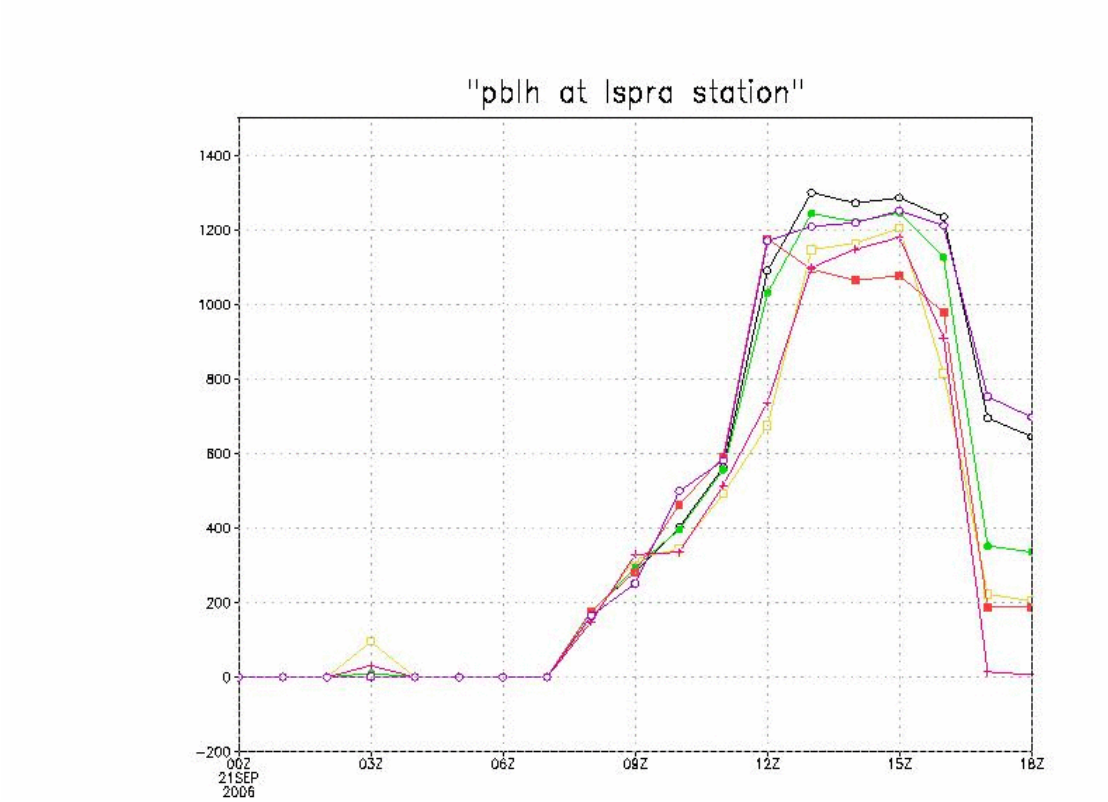

Fig. 6 Boundary layer height: Eta scheme (x-axis: UTC time, y-axis: height [m])

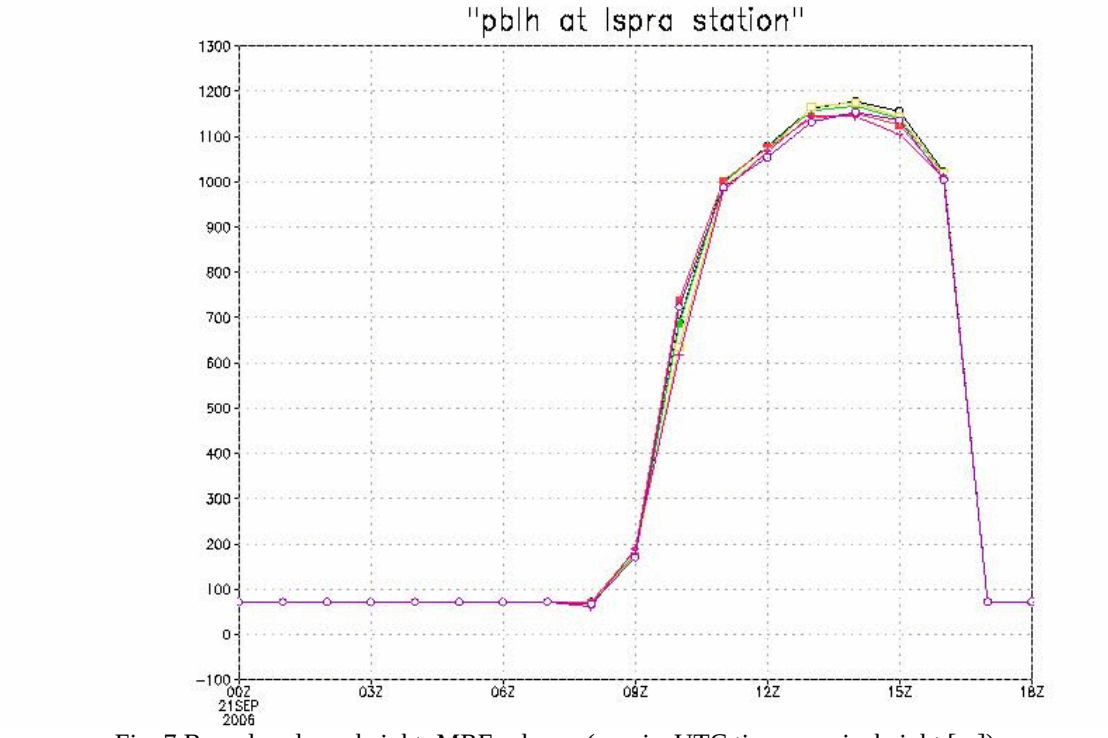

Fig. 7 Boundary layer height: MRF scheme (x-axis: UTC time, y-axis: height [m])

In all the cases maximum is reached approximately between 12.00 and 15.00 at 1100-1200 m. The height starts to grow at about 9.00 and goes down at 17.00 UTC. On the next three pictures (Figs. 8-10) boundary layer height is shown on the map for domain

4 for some selected hours during the day. Discontinuities seen as rectangles on these maps correspond to the regions of glacier or cover of snow or ice.

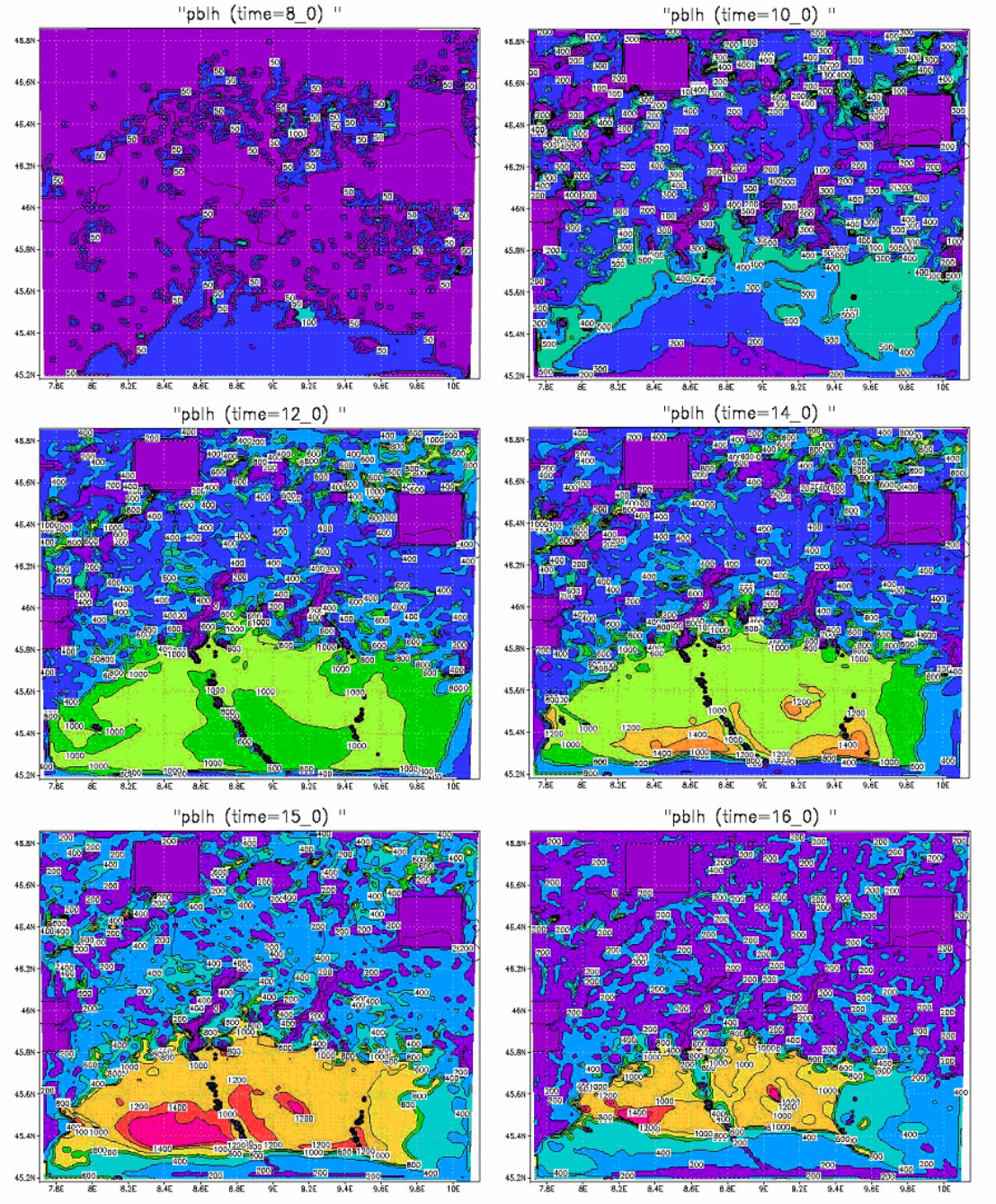

Fig. 8 Boundary layer height: Blackadar scheme (UTC times: 8,10,12,14,15,16)

Blackadar and MRF schemes produced compatible maps, while Eta scheme a little bit different, however the structure is generally similar.

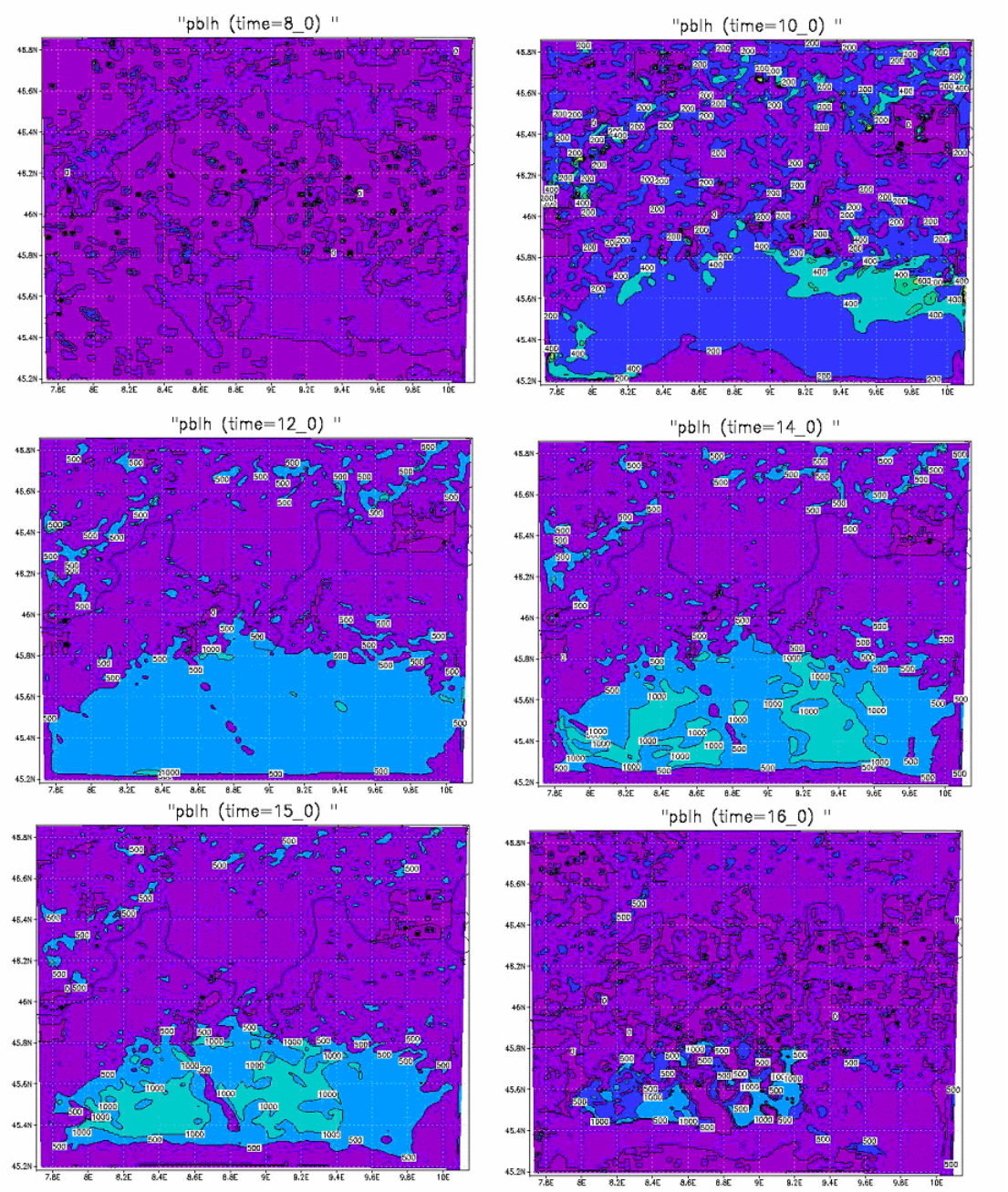

Fig. 9 Boundary layer height: Eta scheme (UTC times: 8,10,12,14,15,16)

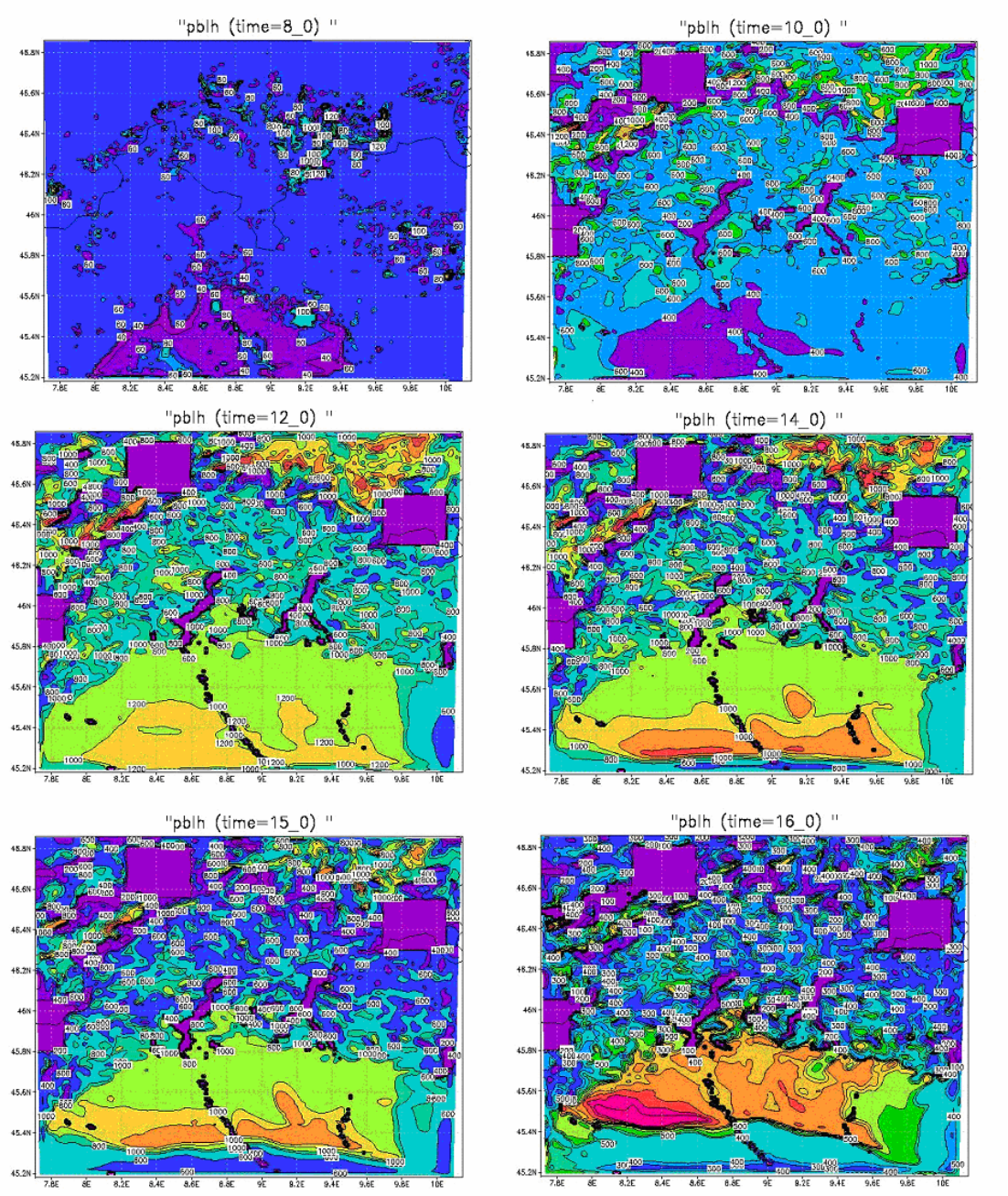

Fig. 10 Boundary layer height: MRF scheme (UTC times: 8,10,12,14,15,16)

In the pictures below time series of sensible heat flux (Figs. 11-13) and friction velocity (Figs. 13-15) are presented. The same colors as for boundary layer were used. The maximum values reached at about 12.00 UTC do not differ substantially.

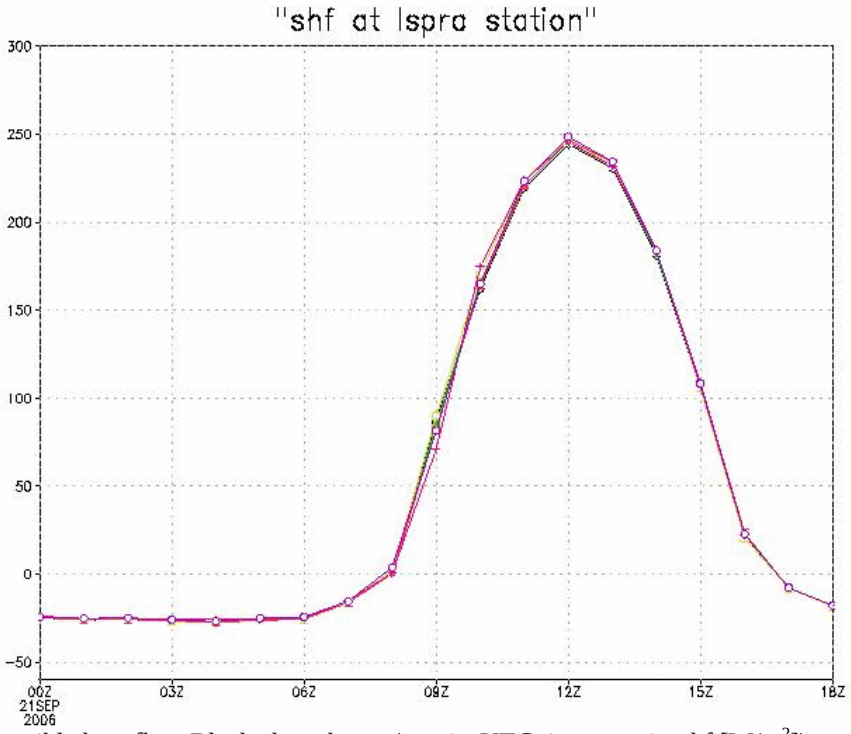

Fig. 11 Sensible heat flux: Blackadar scheme (x-axis: UTC time, y-axis: shf [W/m^2])

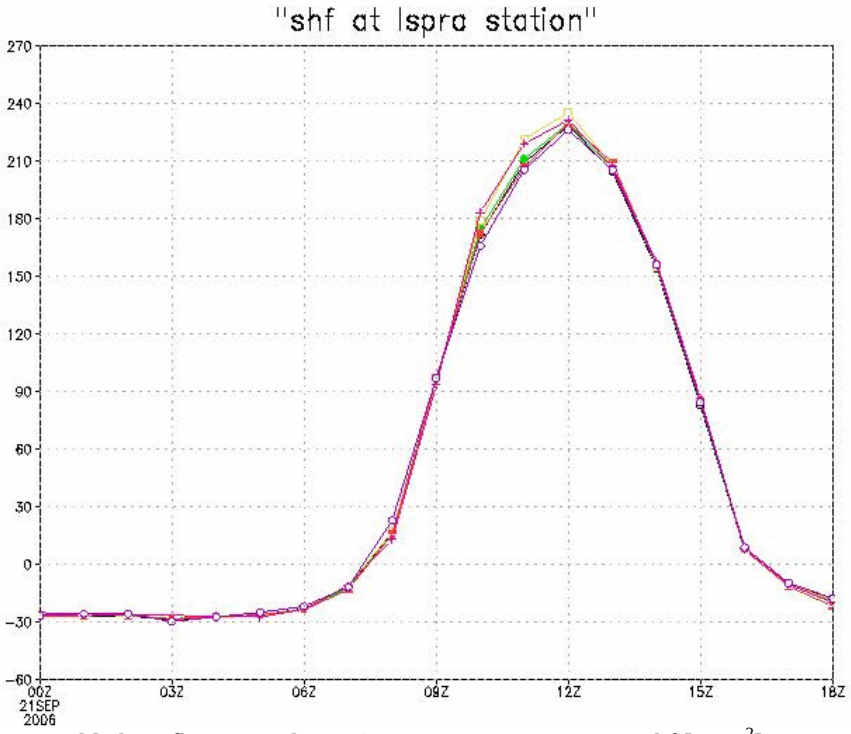

Fig. 12 Sensible heat flux: Eta scheme (x-axis: UTC time, y-axis: shf [W/m^2])

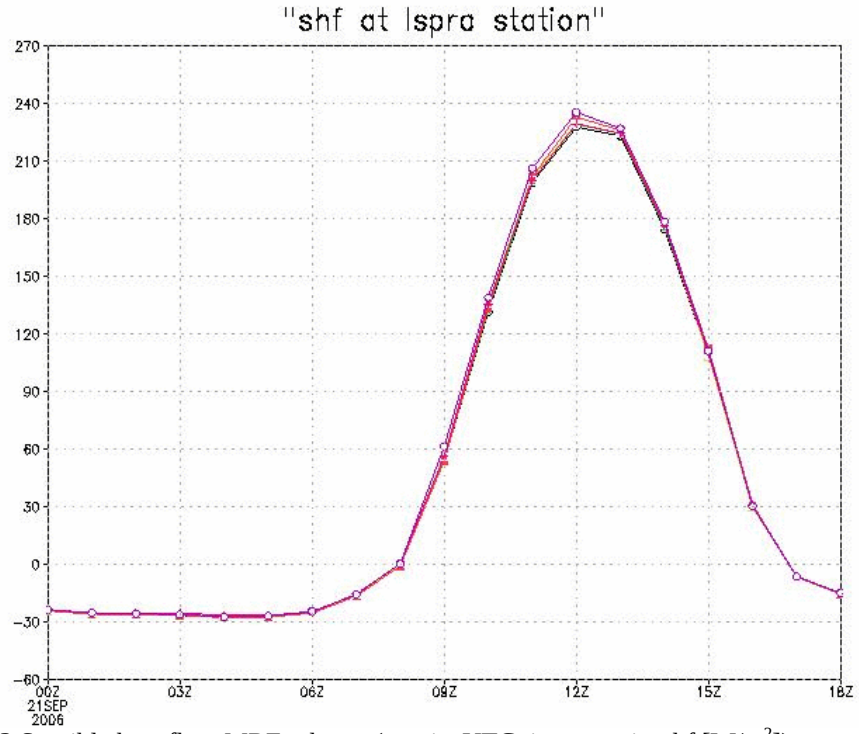

Fig. 13 Sensible heat flux: MRF scheme (x-axis: UTC time, y-axis: shf [W/m^2])

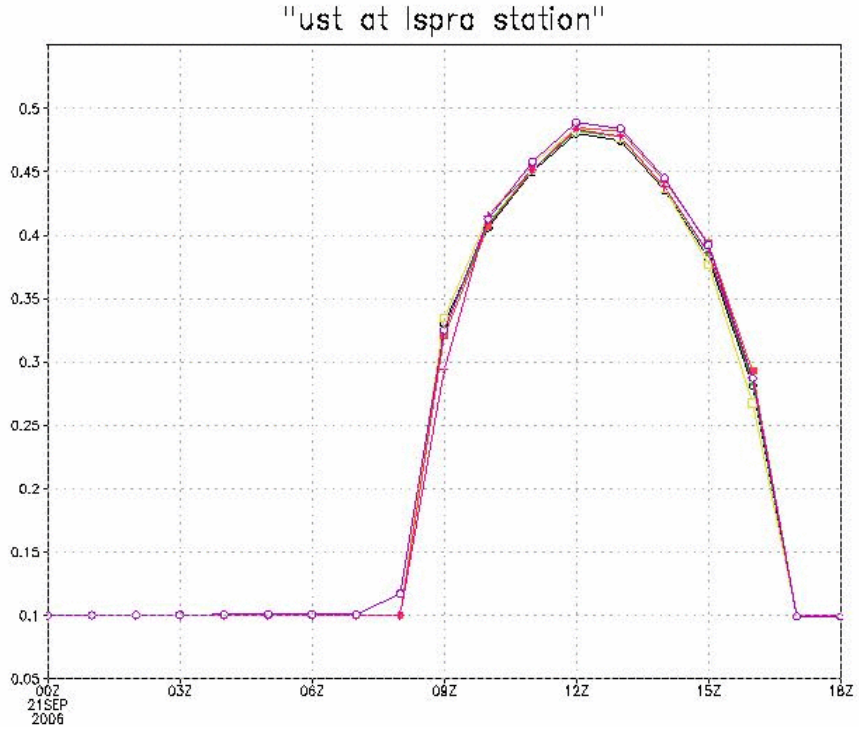

Fig. 14 Friction velocity: Blackadar scheme (x-axis: UTC time, y-axis: ust [m/s])

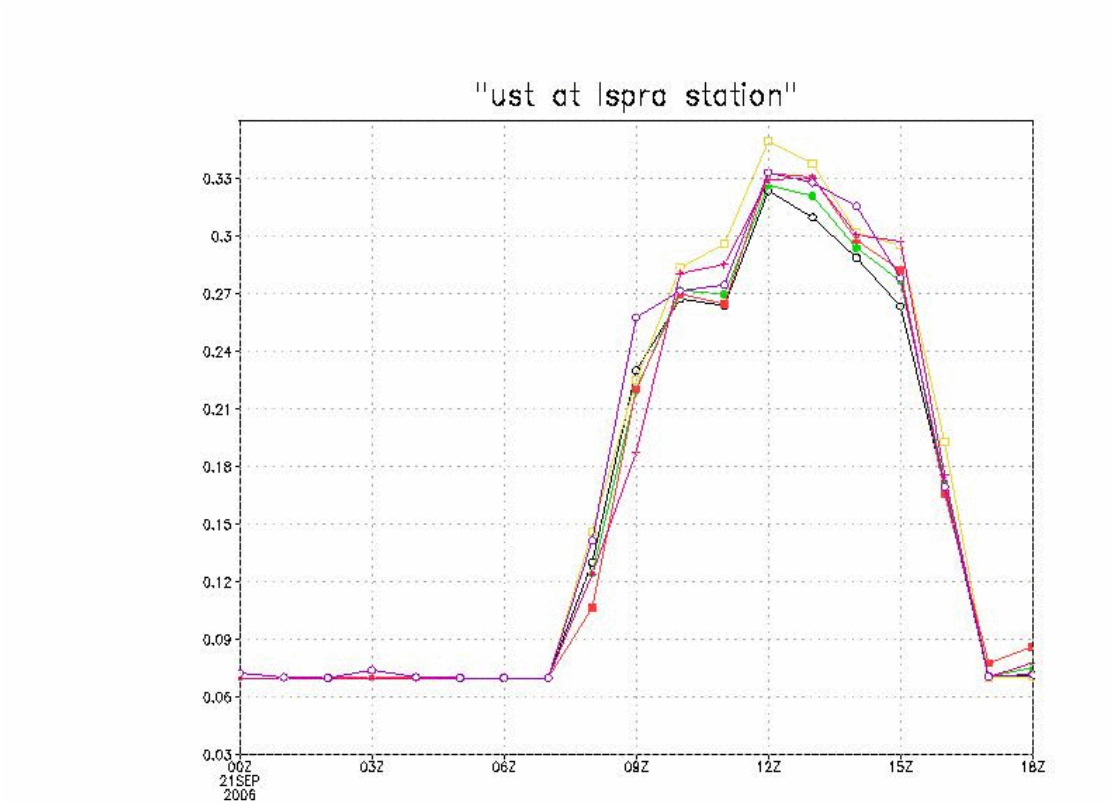

Fig. 15 Friction velocity: Eta scheme (x-axis: UTC time, y-axis: ust [m/s])

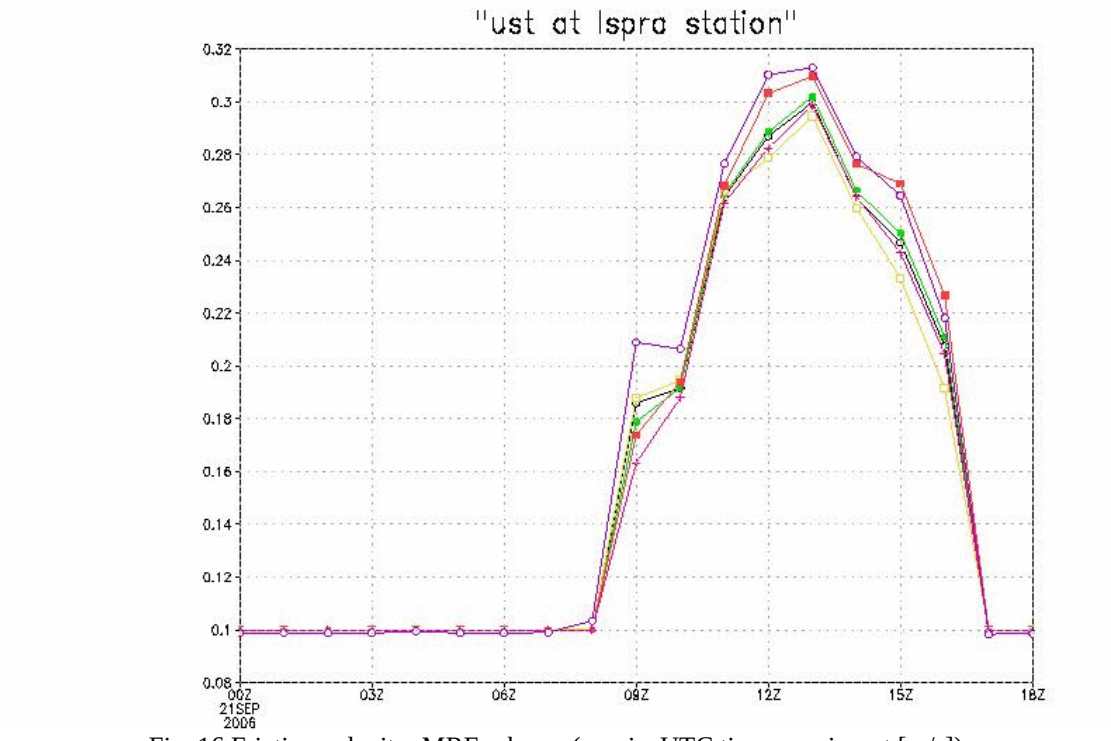

Fig. 16 Friction velocity: MRF scheme (x-axis: UTC time, y-axis: ust [m/s])

Similarly to what done for the boundary layer height, in the following maps sensible heat flux (Figs. 17-19) and friction velocity (Figs. 20-22) are shown for the domain 4. Reasonable agreement for different parameterizations can be observed.

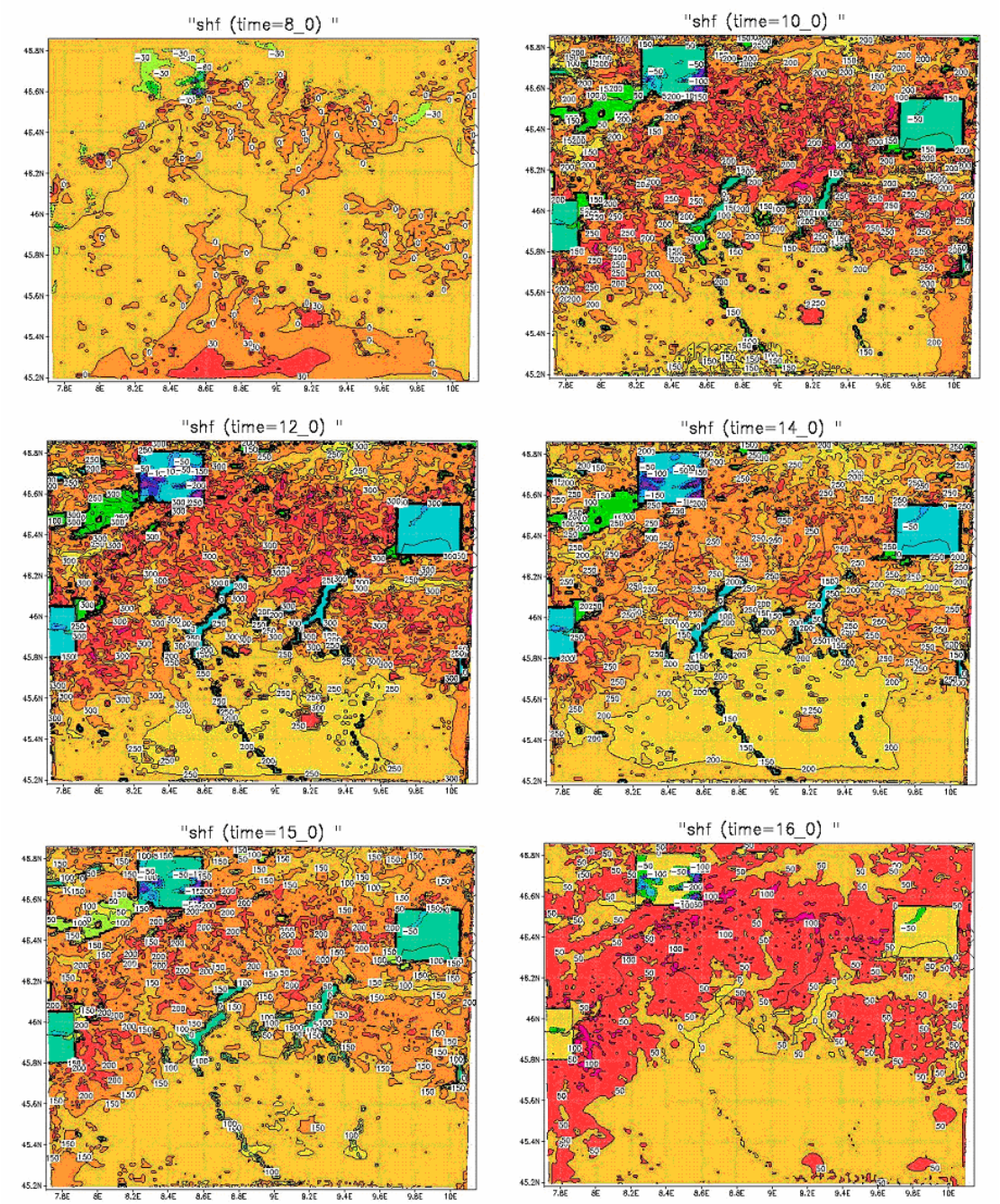

Fig. 17 Sensible heat flux: Blackadar scheme (UTC times: 8,10,12,14,15,16)

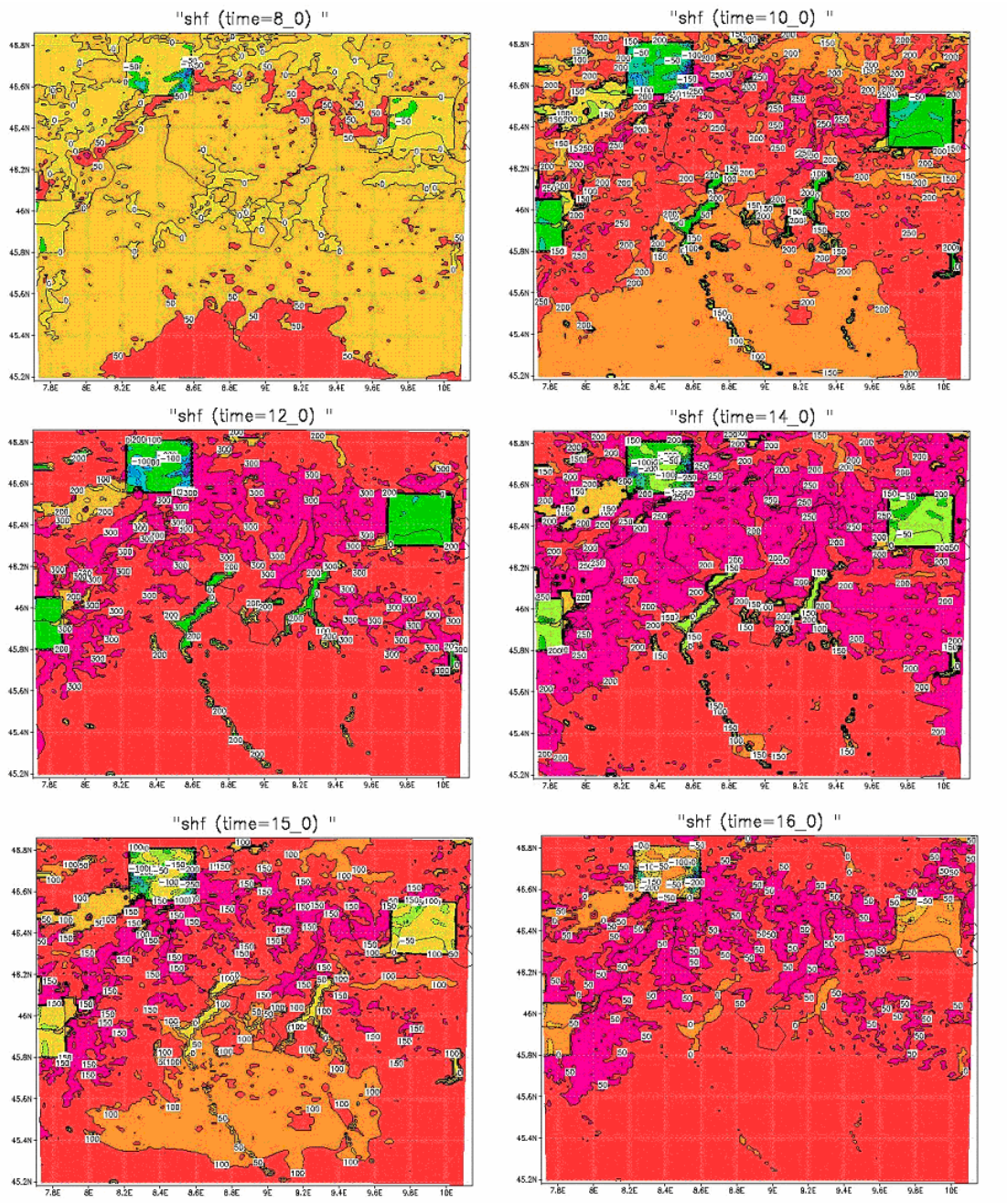

Fig. 18 Sensible heat flux: Eta scheme (UTC times: 8,10,12,14,15,16)

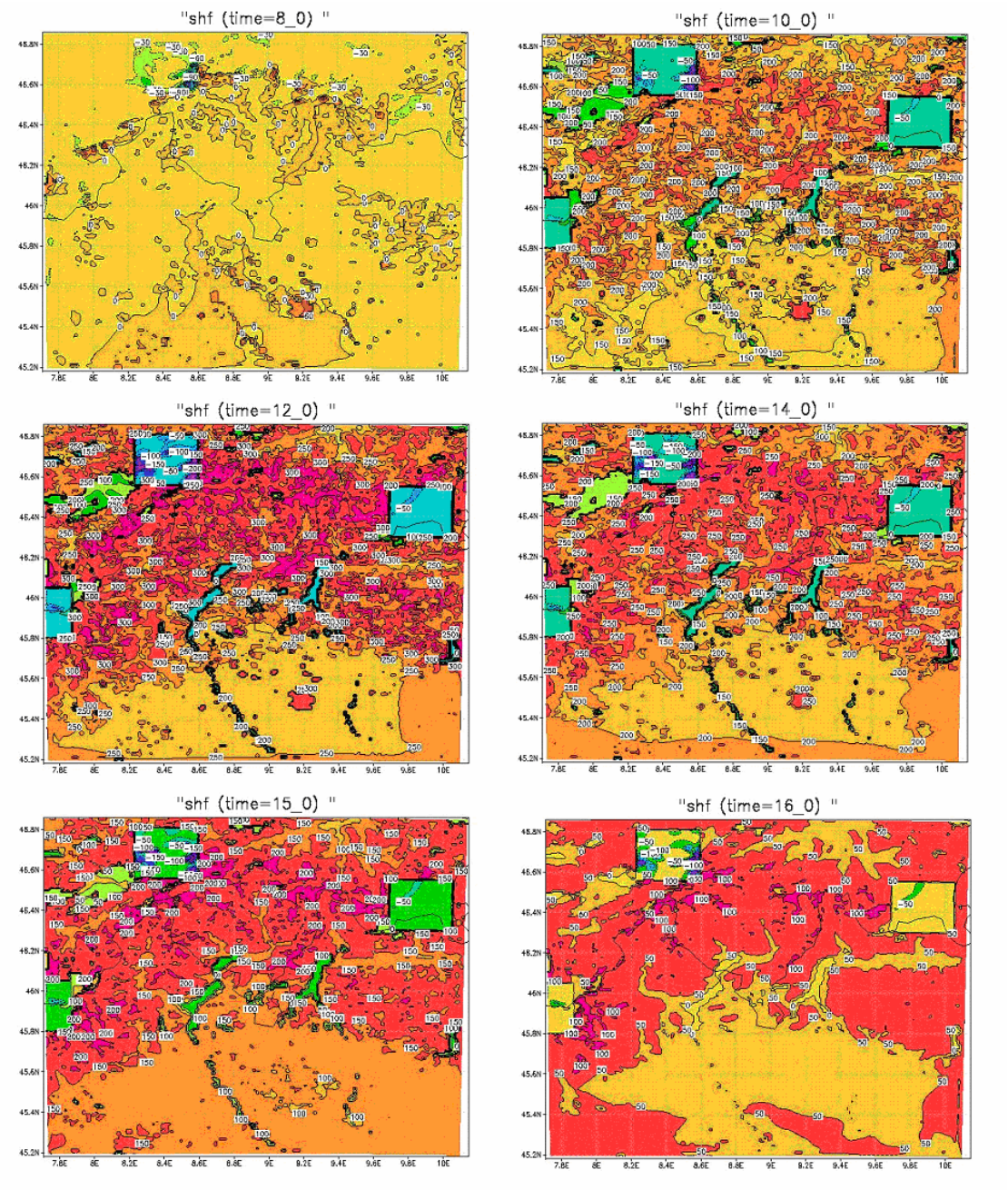

Fig. 19 Sensible heat flux: MRF scheme (UTC times: 8,10,12,14,15,16)

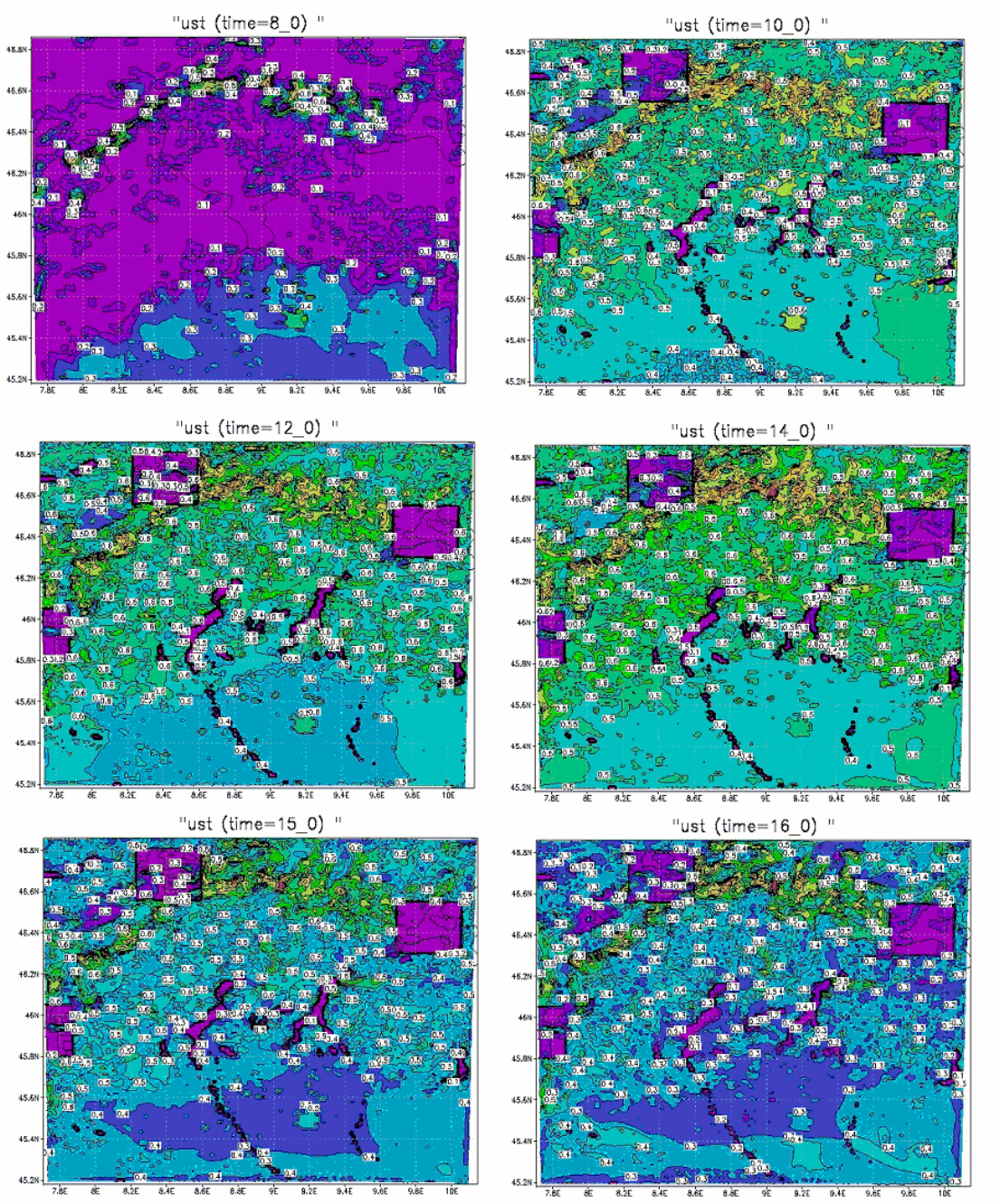

Fig. 20 Friction velocity: Blackadar scheme (UTC times: 8,10,12,14,15,16)

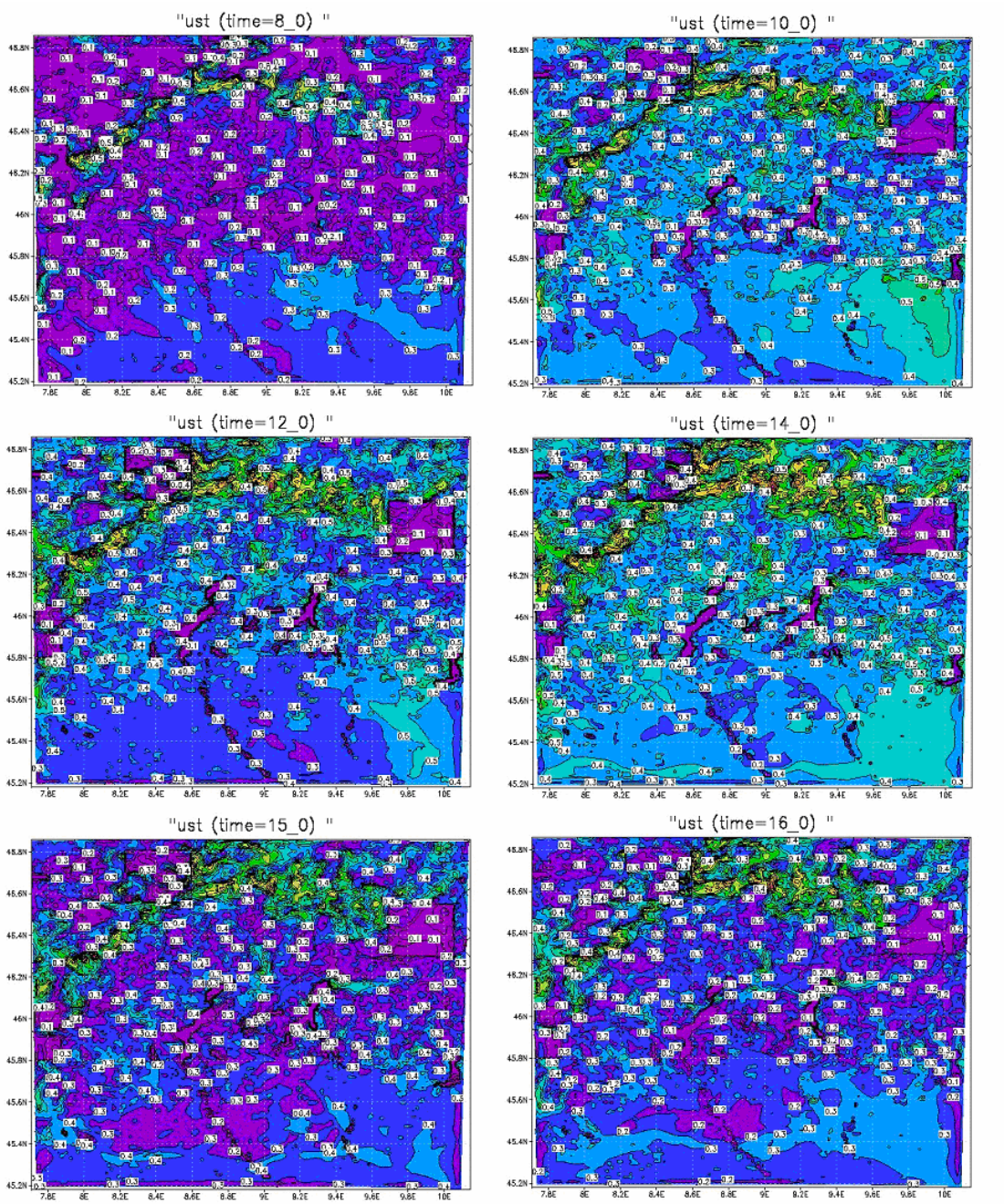

Fig. 21 Friction velocity: Eta scheme (UTC times: 8,10,12,14,15,16)

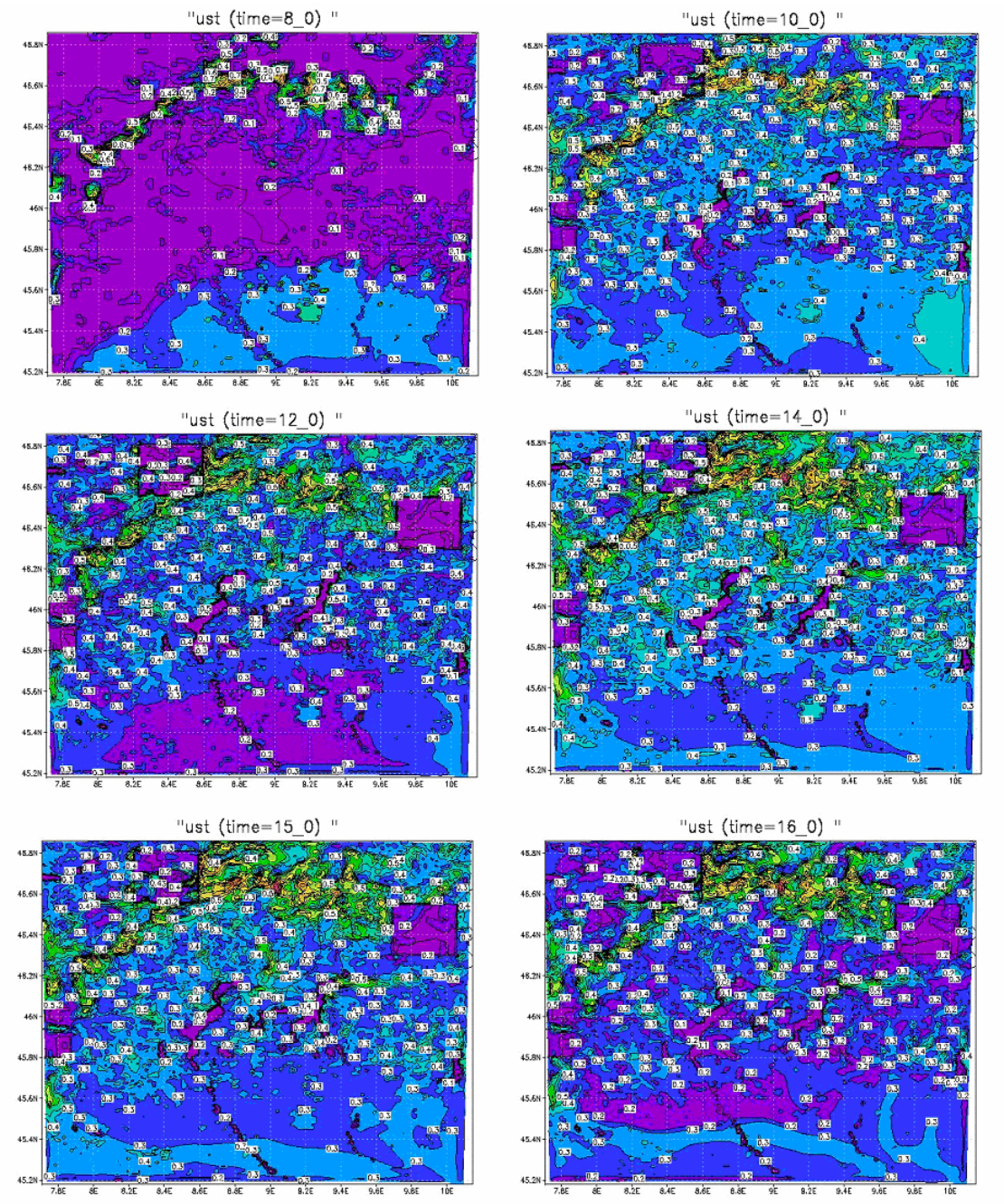

Fig. 22 Friction velocity: MRF scheme (UTC times: 8,10,12,14,15,16)

On the next pictures vertical cross section of the daily wind is shown at Ispra (pressure levels (mb) used for y-axis). Figure 23 shows the total magnitude wind, while Figure 24 the w-wind component. As it can be observed the wind was rather weak, and actually the vertical component could be practically neglected. There were no essential differences between various MM5 runs.

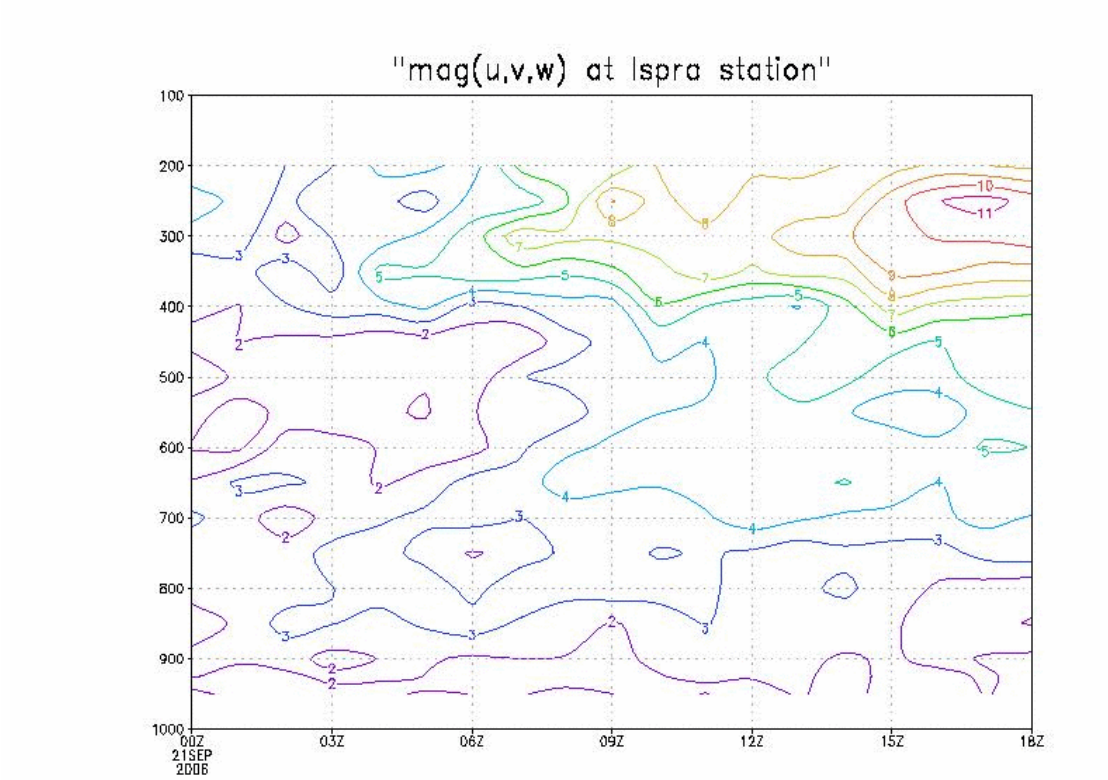

Fig. 23 Vertical cross section of total wind magnitude at Ispra (x-axis: UTC time, y-axis: $\sqrt{u^2+v^2+w^2}$ [m/s])

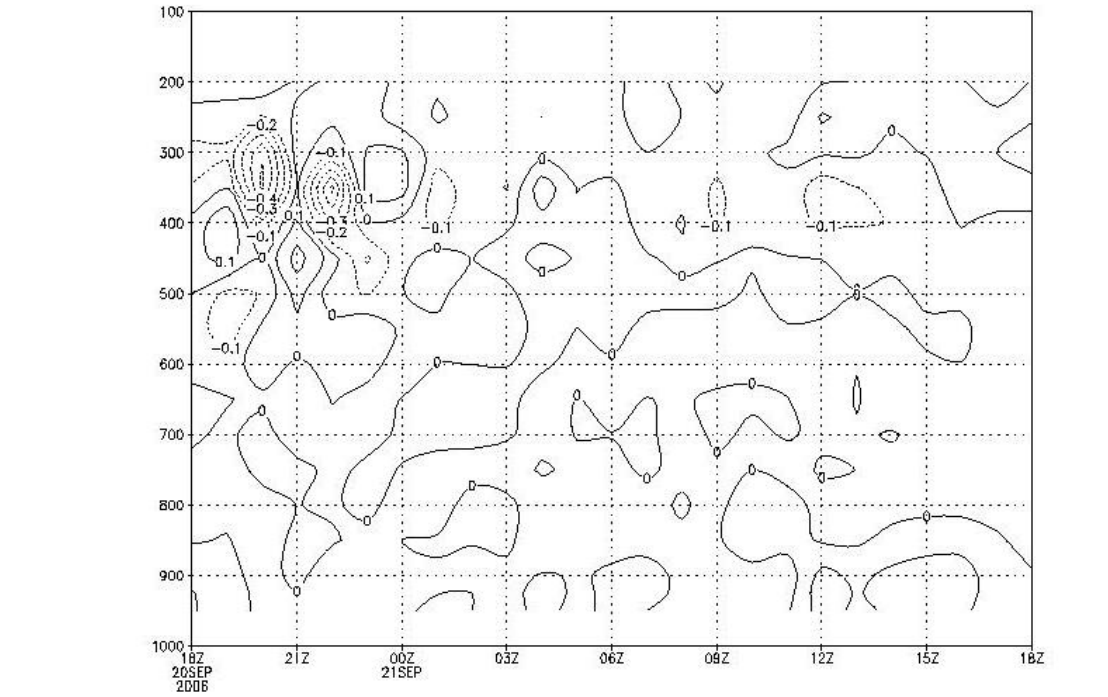

Fig. 24 Vertical velocity at different pressure levels

5. Discussion and Conclusions

The presented results of all simulations show the following effects:

- Negative values of sensible heat flux during the night show that Earth's surface gains energy from the air. At 6 UTC sensible heat flux starts to grow, being positive at about 8 UTC and is increasing fast obtaining maximum at midday. Thus during the day heat energy is transferred from Earth's surface up to the atmosphere. Then it goes down and the cycle is repeated.
- The behaviour of friction velocity is similar – during the day maximum values are greater by factor 3-5 related to the night period. This indicates that kinematic stress is increased, showing possible vertical transfer of horizontal momentum.

Then the changes of the height of boundary layer correspond to the above mentioned effects – the maximum value of about 1200 m can be observed between 12 UTC and 15 UTC.

Looking at the presented maps one can observe that in the morning sensible heat flux is bigger in the south part of the domain (time 8 UTC), then during the day maximum values are in the Alps. Friction velocity, on the other hand has maximum in the Alps region but it can be noticed that the structure is such that in the morning lowest values are between the Alps and south part in the domain, while during the day in the south (except city of Milan).

During the day, boundary layer is higher also in the southern part of the domain.

During the simulation period wind was not strong (1-3 m/s up to 700 mb), although an increase of wind can be observed during the day at the highest levels (Fig. 23).

Figs. 25-26 show the wind field in the Ispra region on the 950 mb level. At 6 UTC (Fig. 25) a flow towards the Lago Maggiore can be observed, but for most of the day the wind was from south to north as shown on Figs. 26 and 27. At higher levels the wind was from north to south at night (shown at 500 mb for 2 UTC on Fig. 28 – time selected for better illustration), while during the day circulation at those levels was also southerly (Fig. 29). This effect is the typical mountain breeze, as during the day higher parts of the mountains warm up faster and during the night they cool faster.

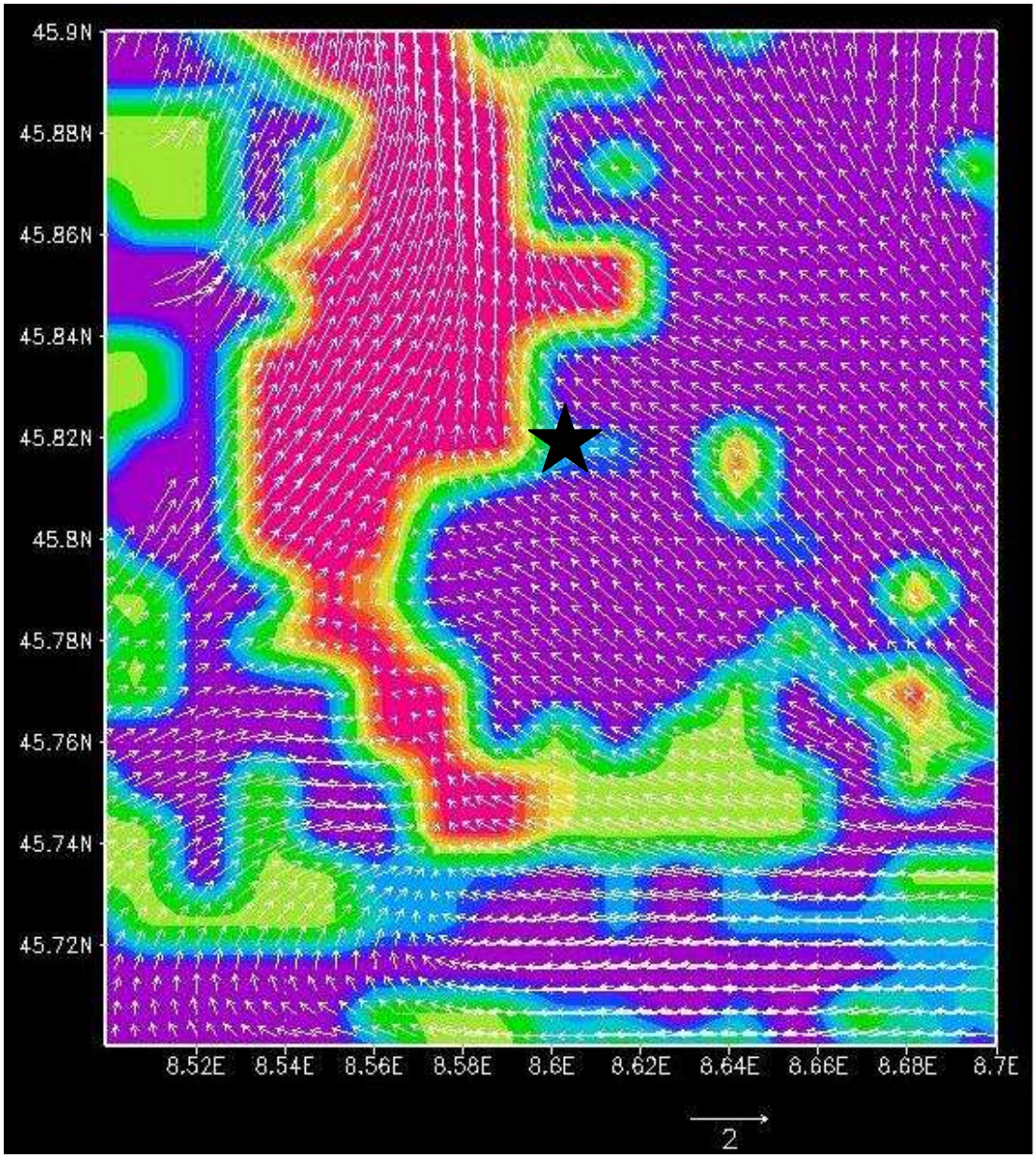

Fig. 25 Wind, 6 UTC level 950 mb (the star indicate the Ispra site, color indicates land use – Lago Maggiore is displayed as red area)

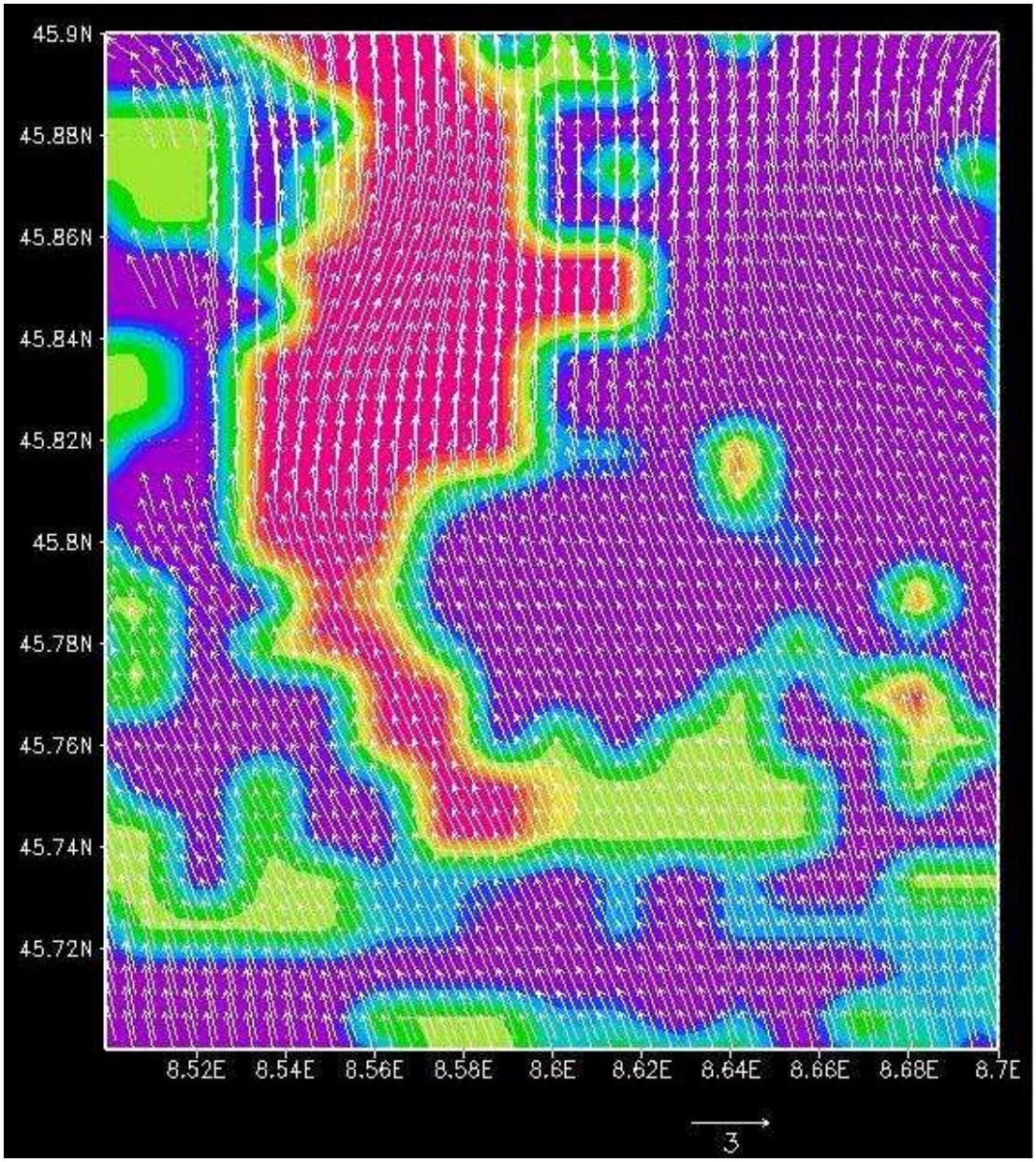

Fig. 26 Wind, 12 UTC level 950 mb

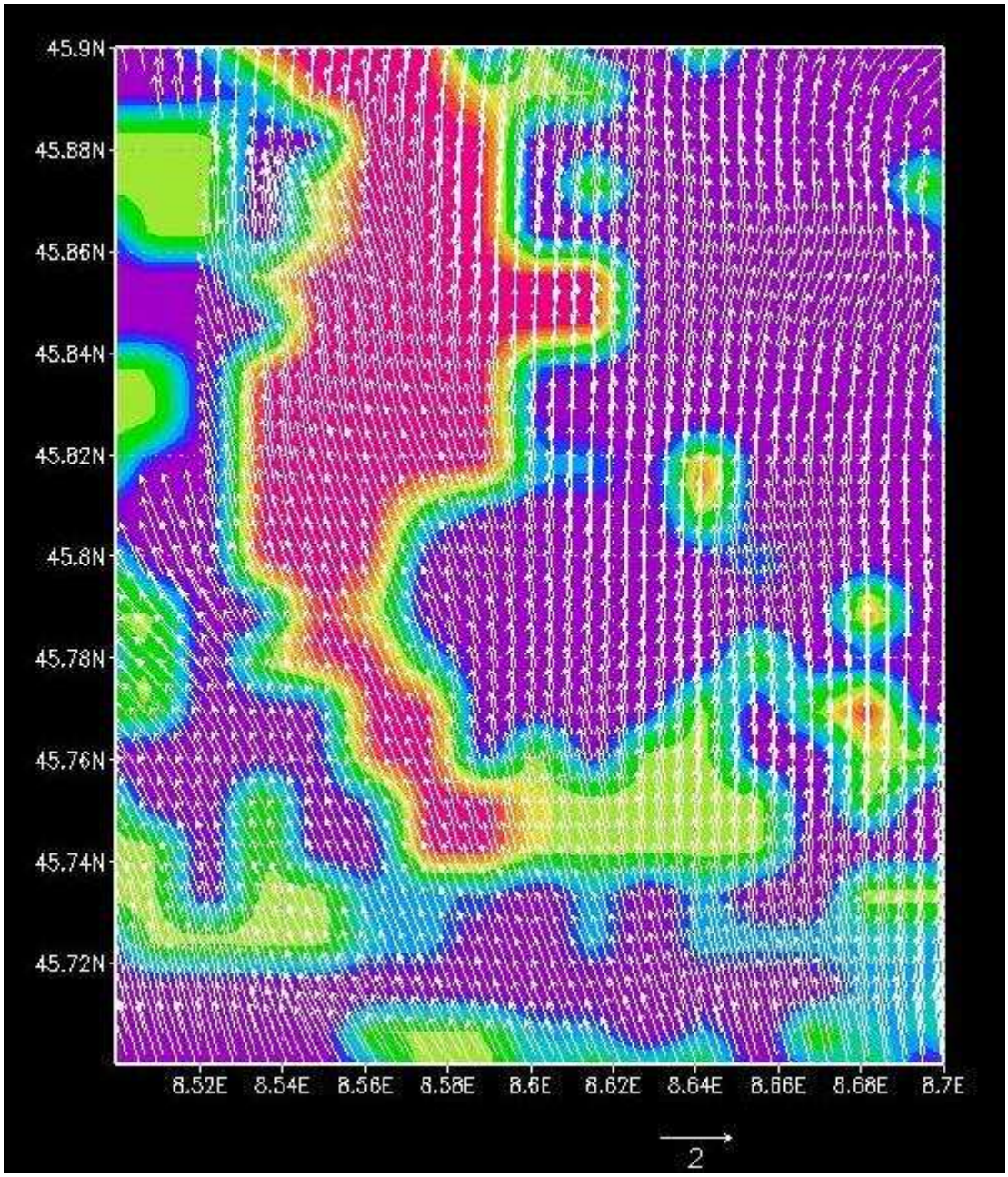

Fig. 27 Wind, 18 UTC level 950 mb

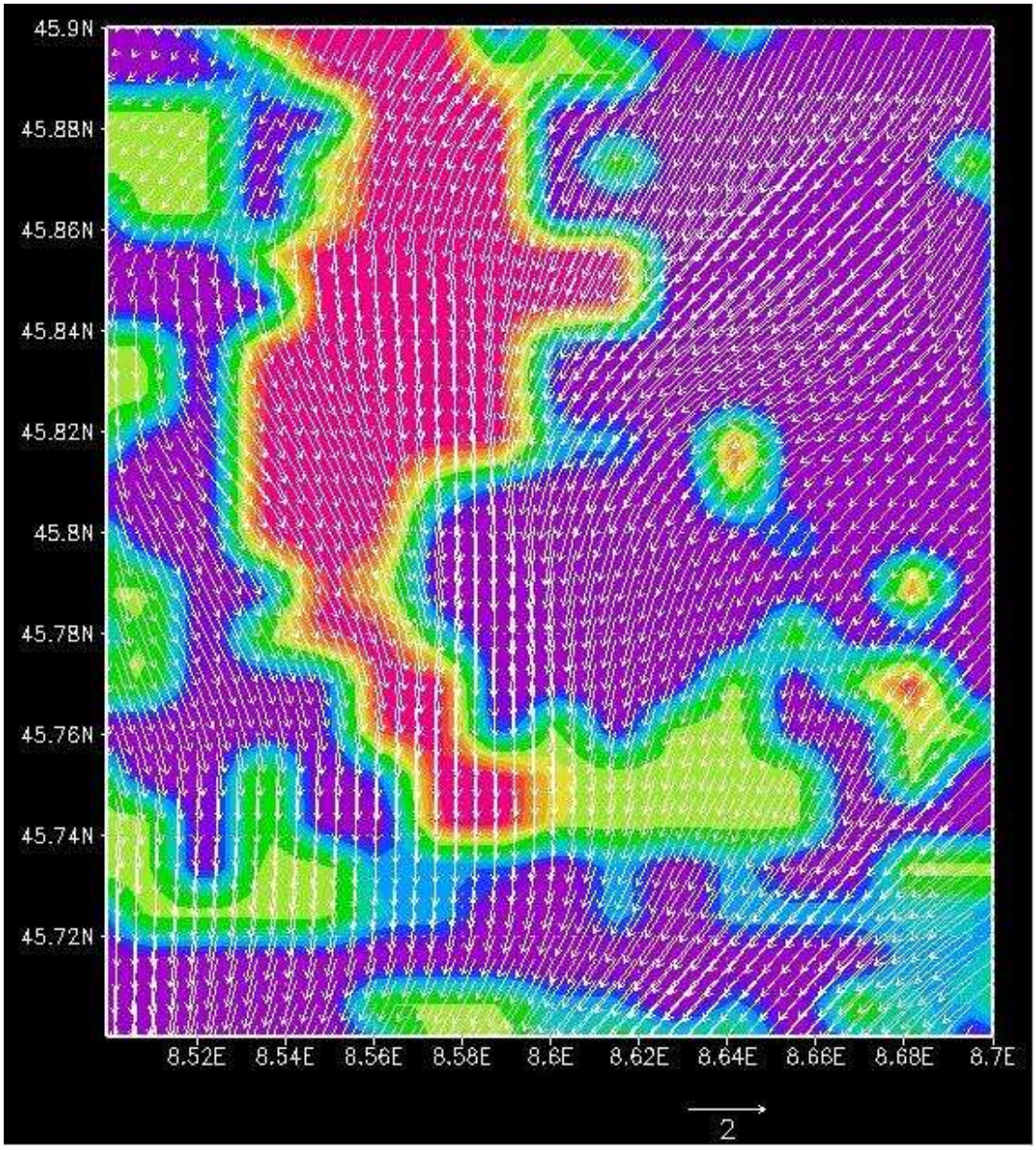

Fig. 28 Wind, 2 UTC level 500 mb

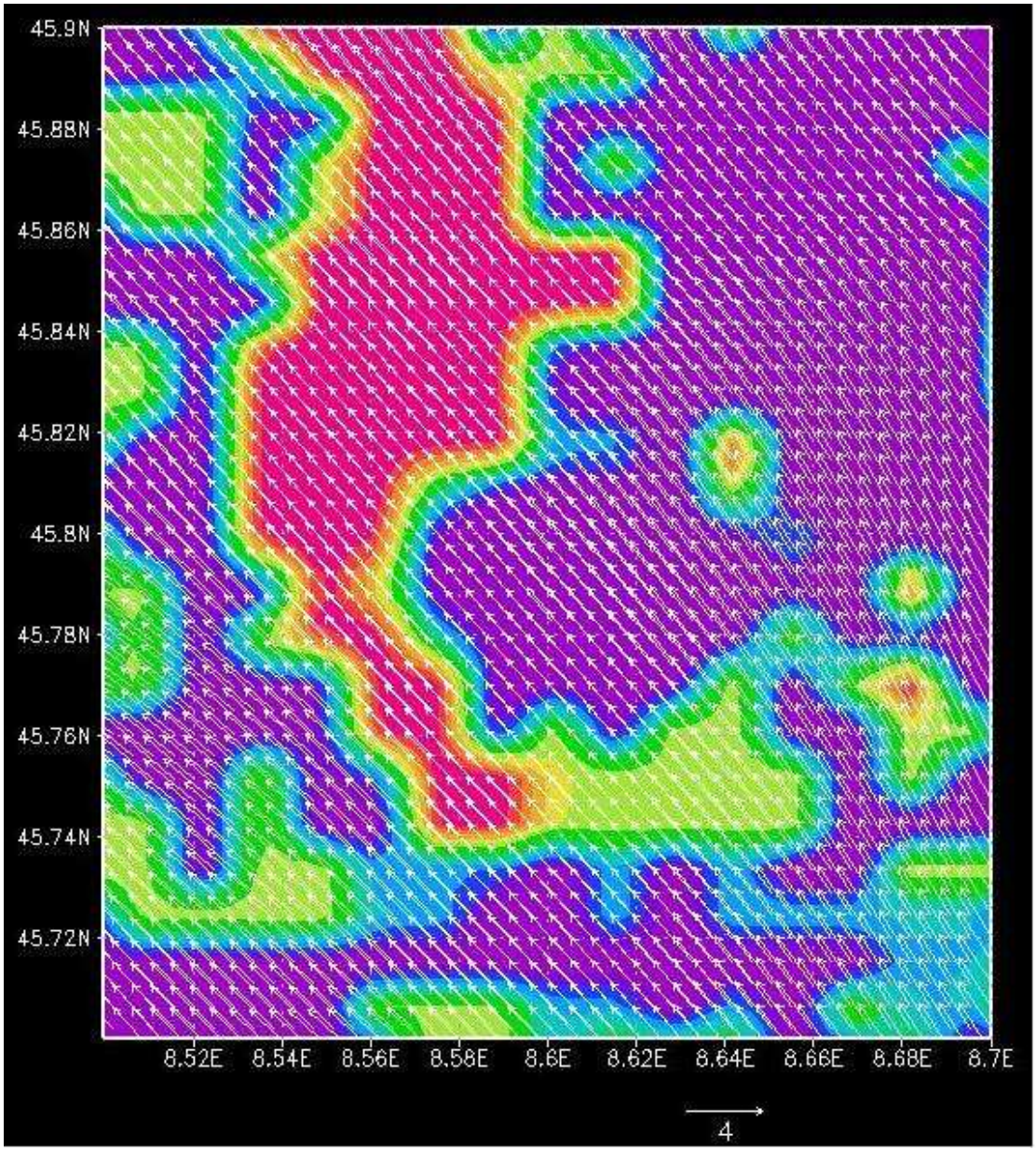

Fig. 29 Wind, 8 UTC level 500 mb

Vertical profile of temperature as a function of time presented on Fig. 30 doesn't show inversion or any anomalies. On the other hand looking more closely at the temperature near ground level (Fig. 31) one can notice inversion near the ground during the night, finishing in the morning, corresponding to time of growth start of boundary layer.

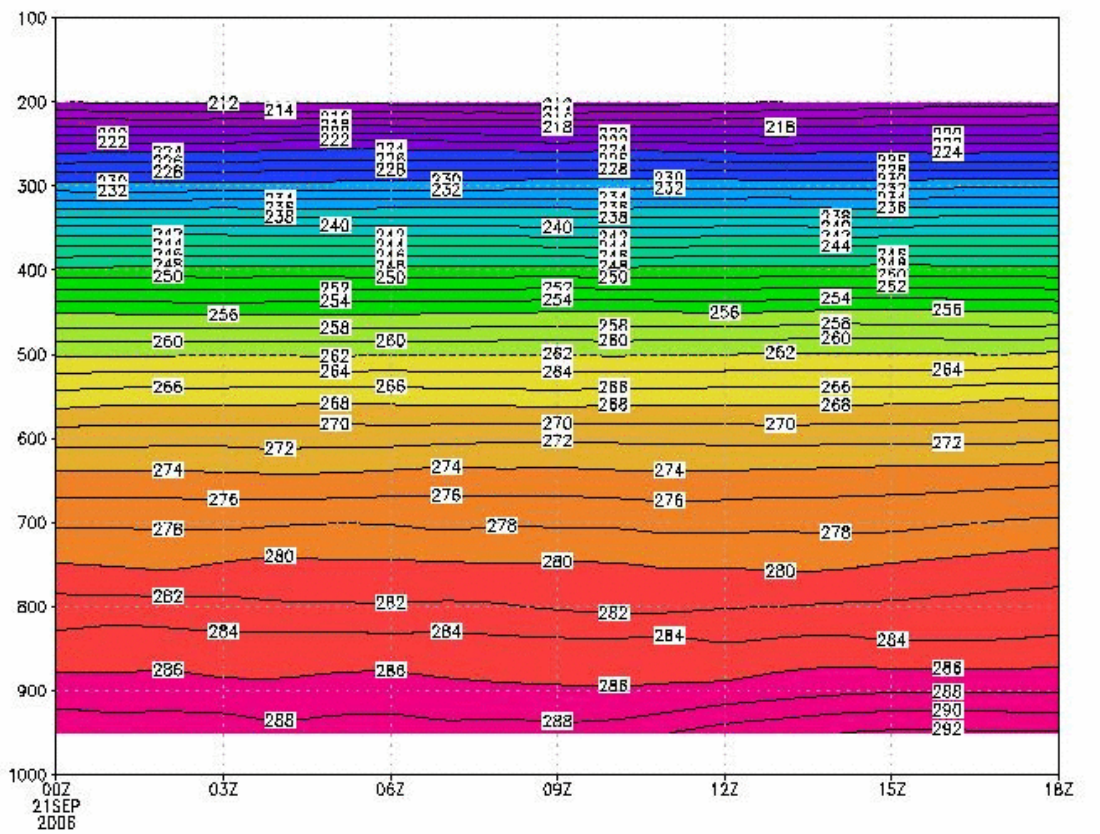

Fig. 30 Temperature at Ispra – vertical profile

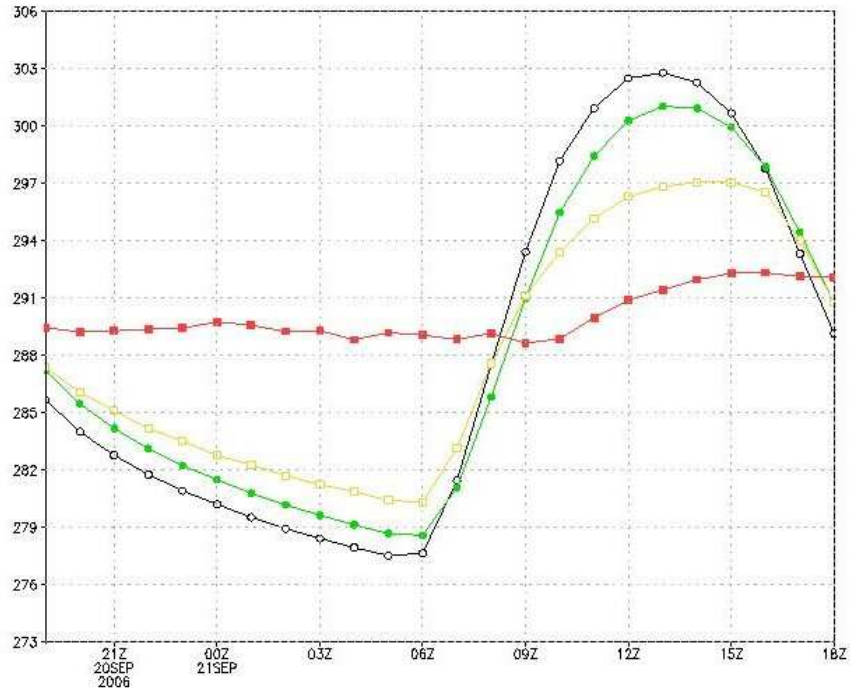

Fig. 31 Temperatures near ground: black – ground, green – soil, yellow at 2 m, red – first vertical level (950 mb – about 65 m above ground)

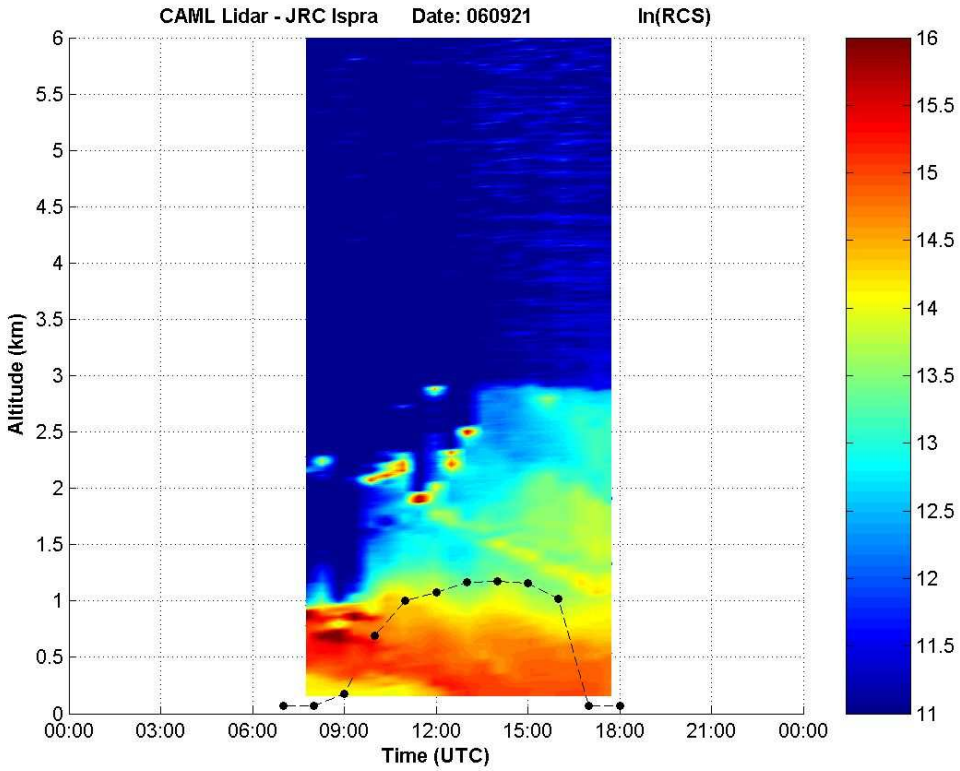

Fig. 32 Boundary layer level (MRF run, black line) visualized on the lidar observations of Fig.1

On Fig. 32 the evolution of the boundary layer height (from MRF run – Fig. 7) is visualized over the lidar observations (Fig.1).

This graph is in some agreement with the lidar picture as:

- the maximum value of boundary height is in a reasonable accordance,
- the shape of the graph, particularly from 11 UTC matches the lidar picture.

Taking into account the fact that:

- weak wind was observed,
- temperature was stratified without anomalies,
- friction velocity and heat flux were typical,

the most likely explanation of the lidar observed aerosol distribution is as follows. A residual layer of aerosol is present aloft (> 300 m) in the first part of the day (< 11 UTC). Then the development of the boundary layer produces a mixing of the lowermost levels. This translates into an enhancement of aerosol in the lowermost levels (as confirmed by independent PM10 measurements performed at the ground, see Fig. 2).

Hence the conclusions can be summarized as follows:

1. Using MM5 and available data sets it is possible to investigate local phenomena in the atmospheric boundary layer (like mountain breeze or ground inversion), but there are some obvious limitations related to the following aspects:
    a. The best resolution of terrain, land use and vegetation data sets is 30 sec, which correspond to about 0.9 km (at middle latitudes). Then – as it was used in described simulation – 1 km grid size is a reasonable choice for high resolution calculations. This in turn means that it can be difficult to simulate some local effects – like impact of the areas, which shape doesn't suit very much to the grid (for example long and narrow lake).
    b. There is a need for appropriate computer power as one can roughly estimate the time needed for making simulations on n nested grid as proportional to the number of grid points times 3 to the (n-1) power (i.e. ~ (number of grid points) x $3^{(\text{number of nested grids } -1)}$). It should be also stressed that putting more advanced physics option makes it necessary to decrease time step to fulfil the Courant-Friedrich-Levy stability condition.
2. The MM5 modelling system has a possibility to include observation data using nudging procedure. In particular it could be of some advantage to add information on vertical profiles. The problem is however such, that requested data are often not available for the area of interest. In general coupling of observational data with high resolution numerical weather simulation is useful if the measured data have good frequency and possible come from at least a few stations in the domain. In this respect the drawback of used lidar station is that there are no nocturnal data.
3. With respect to the original question related to the observed lidar picture on the lidar station there is no clear response. However, one can rather exclude:
    a. Impact of long distance emission source due to weak wind.
    b. Any particular processes in boundary layer like specific convective movements or turbulence.

The observed high concentrations registered in the lowermost levels and at the ground after midday come probably from a mixing of the residual layer from the previous day driven by the boundary layer development.

The analyzed case of 21.09.06 gives just an example of possible coupling between weather numerical modeling and lidar measurements. Further investigations could be performed considering cases of different vertical stratifications. Moreover, cases in which lidar measurements are available 24h per day should be addressed to follow the complete daily cycle.

From a model point of view, the possibility of making higher resolution simulations should be explored.

Bibliography

1. G. Grell, J. Dudhia, D. Stauffer, A Description of the Fifth-Generation Penn State/NCAR Mesoscale Model (MM5), NCAR/TN-398+STR, 1995

2. J. Dudhia, D. Gill, K. Manning, W. Wang, C. Bruyere, PSU/NCAR Mesoscale Modeling System Tutorial Class Notes and Users' Guide *(MM5 Modeling System Version 3)*, 2005

European Commission

EUR 22855 EN – DG Joint Research Centre, Institute for Environment and Sustainability
Title: Numerical weather simulations in support to the CCU CAML Lidar measurements: Preliminary results for the case study of 21st September 2006
Authors: S. Potempski, F. Barnaba, S. Galmarini
Luxembourg: Office for Official Publications of the European Communities
2007 – 31 pp. – 21 x 29.7 cm
EUR - Scientific and Technical Research series; ISSN 1018-5593

Abstract

The report describes a series of weather numerical mesoscale simulations performed in high resolution to understand to which extent the lidar-detected evolution of the particles distribution along the vertical could be explained by the boundary layer and/or horizontal transport processes. A particular stress was put on investigation of boundary layer parameters. The case study of 21st September was chosen for simulations, when the CCU-CAML lidar at Ispra registered quite high values of aerosols up to 1 km altitude, and the lidar revealed a descent of the highest aerosol loads towards the ground during the morning.

EUROPEAN COMMISSION
DIRECTORATE-GENERAL
Joint Research Centre

The mission of the JRC is to provide customer-driven scientific and technical support for the conception, development, implementation and monitoring of EU policies. As a service of the European Commission, the JRC functions as a reference centre of science and technology for the Union. Close to the policy-making process, it serves the common interest of the Member States, while being independent of special interests, whether private or national.